

ATMS: Algorithmic Trading-Guided Market Simulation

Song Wei^{†,*}, Andrea Coletta[†], Svitlana Vyetrenko[†], and Tucker Balch[†]

[†]J.P. Morgan AI Research, ^{*}Georgia Institute of Technology.

Abstract

The effective construction of an Algorithmic Trading (AT) strategy often relies on market simulators, which remains challenging due to existing methods' inability to adapt to the sequential and dynamic nature of trading activities. This work fills this gap by proposing a metric to quantify market discrepancy. This metric measures the difference between a causal effect from underlying market unique characteristics and it is evaluated through the interaction between the AT agent and the market. Most importantly, we introduce Algorithmic Trading-guided Market Simulation (ATMS) by optimizing our proposed metric. Inspired by SeqGAN, ATMS formulates the simulator as a stochastic policy in reinforcement learning (RL) to account for the sequential nature of trading. Moreover, ATMS utilizes the policy gradient update to bypass differentiating the proposed metric, which involves non-differentiable operations such as order deletion from the market. Through extensive experiments on semi-real market data, we demonstrate the effectiveness of our metric and show that ATMS generates market data with improved similarity to reality compared to the state-of-the-art conditional Wasserstein Generative Adversarial Network (cWGAN) approach. Furthermore, ATMS produces market data with more balanced BUY and SELL volumes, mitigating the bias of the cWGAN baseline approach, where a simple strategy can exploit the BUY/SELL imbalance for profit.

Keywords: Agent-Based Simulation, Causal Inference, Deep Generative Model, Reinforcement Learning, Stock Market Simulation.

*This work was done while S. Wei was interning at J.P. Morgan AI Research. Contact the authors at: song.wei@gatech.edu, {andrea.coletta,svitlana.s.vyetrenko,tucker.balch}@jpmchase.com.

1 Introduction

Algorithmic trading (AT), as a critical component in numerous financial tasks such as optimal execution, oftentimes relies on live interaction with the market, be it real or synthetic, for constructing and testing strategies [Pardo, 2011, Balch et al., 2019]. This live interaction overcomes the limitation of traditional offline methods using historical replays, which fails to capture the dynamic nature of the market, or rather, the response from other market participants, referred to as *background agents*, to AT agent’s action [Coletta et al., 2023]. However, interaction with real market is expensive and rarely feasible for research purpose, thus the most prevalent approach is through the interaction with a *market simulator*, i.e., a generative model aiming to simulate realistic market data. Since the market simulator aims to capture the strategies of the background agents, we will use terms “background agent(s)” and “market” interchangeably.

Generative Adversarial Network (GAN) [Goodfellow et al., 2014] is the most prominent market simulator (see Section 1.1 for related works). Specifically, the state-of-the-art (SOTA) approach is conditional Wasserstein GAN(cWGAN) trained on market replays, which was recently proposed by Li et al. [2020], Coletta et al. [2021, 2022]. To the understanding of the authors, the success of cWGAN as SOTA in market simulation comes from its adaption to this specific application: On one hand, by conditioning on the market input, cWGAN captures historical dependence and attempts to adapt to the sequential nature of trading activities (or rather, the interactions among market participants). On the other hand, by using Wasserstein distance as the discriminator (or metric), cWGAN allows synthetic market data that is unseen in the historical real market, potentially improving its generalization ability to account for the complex market dynamics.

However, the aforementioned adaptations are still less than satisfactory. *First, cWGAN only considers sequential trading activities locally.* Specifically, we use s and a to denote the market state input to the AT agent and the corresponding action, and y and x to denote the market state input to the background agent and the corresponding action. Loosely speaking, the trading process can be represented by the chain structure with snapshot $s_{t-1} \rightarrow a_t \rightarrow y_t \rightarrow x_t \rightarrow s_t$ at time step t (please refer to Section 2 for rigorous definitions of notations and Figure 1 for detailed trading process illustration). However, cWGAN only accounts for $y_t \rightarrow x_t$ part of the above snapshot within time step t , as it employs the classic metric (or loss function), i.e., the Wasserstein distance, to penalize the discrepancy between synthetic and real background agents’ actions for given market input — the classic metric is

local. Moreover, cWGAN models the state-action pairs (i.e., part of the above snapshots) independently — the model formulation is local and fails to account for the sequential nature behind those pairs; Indeed, GAN has been most widely used for image data [Pan et al., 2019, Jabbar et al., 2021], whereas the application to sequential data, including speech, text and orders in stock market, needs careful attention and adaption, such as SeqGAN [Yu et al., 2017].

The second pitfall of cWGAN is its poor generalization ability, which comes from the offline training on replays: Coletta et al. [2023] recently revealed that although cWGAN achieves SOTA realism in isolation (i.e., no external AT agent during the simulation), it may not respond realistically when there exists external agent aggressively placing orders that create unseen (during its training) market states. Consequently, the cWGAN’s response (which shapes the simulated market) to those unseen states becomes unrealistic. Even though using Wasserstein distance as the metric allows cWGAN outputs that are unseen in reality, training on replays cannot introduce unseen market states to improve the generative model’s robustness and factuality. Therefore, it is crucial to introduce external AT agents and consider the live/online interaction between external and background agents during the training, which can capture the market dynamics and improve simulator resilience under unseen and rare market states [Coletta et al., 2023]. To the knowledge of the author, even though there are many recent efforts on GAN-based market simulators (to be reviewed in Section 1.1), they did not go beyond either the classic local metric or offline training on replays. In particular, just like the application of GAN in text or language generation [Zhang et al., 2017], a satisfying quantitative metric that adapts to the sequential, complex, and dynamic natures of the trading market is largely missing [Bouchaud et al., 2018, Vyetrenko et al., 2020], rendering it challenging to train generative models that output realistic market data.

In this work, we address the aforementioned issues by proposing a market distance metric that accounts for the sequential and dynamic nature of the trading activities, based on which we develop an online training scheme. As illustrated in Figure 1, our approach only requires offline interactions/replays of the real-world AT agent with the real market, and thus will not interfere with the real-world production; The training scheme is online because the objective function, or rather the proposed market distance metric, is obtained through the online interaction, which we call *rollout*, of the real-world AT agent with the synthetic market. Specifically, we identify the causal effect [Rubin, 1974] from the background agents during the rollout as the unique characteristic of the underlying market and take the difference between the characteristics under real and synthetic markets as our market distance metric. Inspired

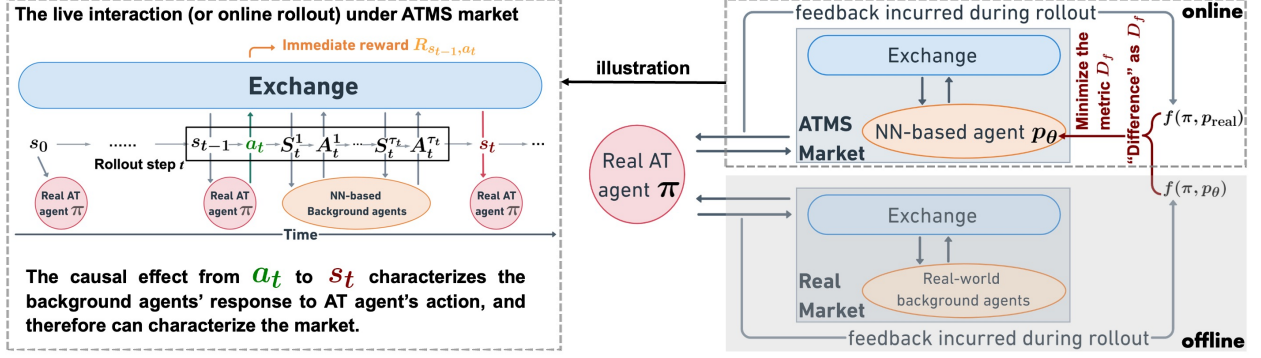
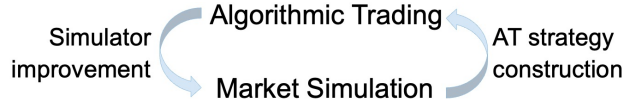


Figure 1: Illustration of the AT agent’s interaction with the market, i.e., rollout, (left) and the ATMS training (right). The market consists of background agents and the exchange. As in both real and simulated markets, within the t -th step, the background agents act τ_t times, i.e., place τ_t orders, between two consecutive wake-ups of the AT agent.

by SeqGAN [Yu et al., 2017], we formulate the generator network as a stochastic policy to account for the sequential nature of the market simulation. Moreover, by leveraging the Policy Gradient Theorem [Sutton et al., 1999], we propose Algorithmic Trading-guided Market Simulation, referred to as *ATMS*, that minimizes our proposed metric to train the generator network without differentiating our metric, since its evaluation involves non-differentiable operations such as order deletion. Through extensive experiments on semi-real market data [Byrd et al., 2020, Amrouni et al., 2021], we show that our approach can generate much more realistic market data compared with the cWGAN-based market simulator. This improvement



could in turn facilitate the use of sample inefficient RL approaches for AT strategy construction, reducing “time-period bias” and the unrealistic reactivity of existing cWGAN-based simulators. Furthermore, while in this paper we specifically focus on simulating financial stock markets, our approach has broad applicability in all environments with interacting agents, including language model [Bai et al., 2022] and traffic simulation for self-driving algorithm development [Suo et al., 2021].

1.1 Literature

In this subsection, we review recent developments in market simulation. We defer an extended literature survey to Appendix A due to space consideration.

Training experimental AT agents usually involves interaction with the real market, which is often impractical. To create a suitable market for the AT agent, generative models representing all background agents are needed and have gained prominence in finance, with GAN being a particularly popular choice. To the knowledge of the author, this line of research traces back to [Kumar et al. \[2018\]](#), [Shi et al. \[2019\]](#), who adapted GAN to generate BUY orders in e-commerce markets. More importantly, GAN has been utilized to model more complex stock markets and simulate various types of stock market data, including transaction event time [[Xiao et al., 2017, 2018](#)], price [[Zhang et al., 2019](#), [Da Silva and Shi, 2019](#), [Wiese et al., 2020](#), [Koshiyama et al., 2021](#)], and even orders [[Li et al., 2020](#), [Coletta et al., 2021, 2022](#)].

Specifically, this work considers Limit Order Book (LOB) stock market simulation, a field initially studied via Interactive Agent-Based Simulation [[Macal and North, 2005](#)] that models and simulates interactions among background agents, i.e., market participants. Presently, the SOTA parametric approach is Agent-Based Interactive Discrete Event Simulation (ABIDES) [[Byrd et al., 2020](#), [Amrouni et al., 2021](#)]. As mentioned earlier, the adaption to the unique characteristics of the underlying application is crucial to the success of generative models; However, oftentimes it would be too difficult to explicitly describe those rules, especially for trading activities, leading to the application of advanced machine learning techniques to summarize those rules from data — Even within the domain of traffic simulation where agents need to obey strict and explicit traffic rules, parametric approaches incorporating those rules [[Quinlan et al., 2010](#)] are getting replaced by advanced machine learning techniques, such as imitation learning (IL) [[Torabi et al., 2018](#), [Suo et al., 2021](#)]. Under the context of LOB market simulation, precisely specifying the type (momentum agents, value agents, noise agents, etc.) and quantity of background agents to emulate real multi-agent systems is rather challenging. Thus, there are increasing amounts of works replacing parametric models with easy-to-tune neural networks (NNs) to effectively capture the trading market’s complex dynamics, which offers a more flexible and scalable framework for training a generative model to capture the complex market dynamics. The mainstream approach to address this issue is to replace parametric models with easy-to-tune neural networks (NNs), which can effectively capture the trading market’s complex dynamics, and offer a more flexible and scalable framework for training a generative model. Notably, Stock-GAN [[Li et al., 2020](#)] utilized conditional Wasserstein GAN (cWGAN) to generate limit orders; Later, [Coletta et al. \[2021, 2022\]](#) extended Stock-GAN and introduced the concept of a *world agent* (in resemblance to the world model [[Schmidhuber, 2015](#)]), which can not only place limit and

market orders, but also cancel and replace orders.

The aforementioned GAN-based approaches explored various NN architectures, trying to adapt to the corresponding applications, but none of them went beyond the classic local loss that directly penalizes the action of background agents (i.e., the output of the generator) for given input market state — one exception is [Shi et al. \[2019\]](#), where they studied the customer/agent policy, i.e., how to place BUY orders in the e-commerce market, with reinforcement learning (RL), and leveraged adversarial imitation learning [[Ho and Ermon, 2016](#), [Torabi et al., 2018](#)] that replaced the critic in GAN with the agent reward. On one hand, as the generative model tries to capture the policy of the background agents, it is natural to use RL or IL. In the same spirit of our adaptation of SeqGAN, [Shi et al. \[2019\]](#) used IL for generator training to account for the sequential nature of the market. However, to the best of our knowledge, [Shi et al. \[2019\]](#) seems to be the only attempt along the direction of IL for market simulation. On the other hand, as we will see in Section 4, using the reward directly as the loss cannot capture the causal relationship that is able to discriminate real and synthetic markets; additionally, [Shi et al. \[2019\]](#) has limitations as it can only place one type of orders.

Table 1: Comparison between cWGAN and ATMS: the first two rows correspond to the sequential nature of the trading activities whereas the online/offline training is related to the complex dynamics of the trading market.

cWGAN	ATMS
Local metric: Wasserstein distance	Interactive AT-based metric
Local model: GAN	Generator formulated as RL policy: SeqGAN
Offline training with market replay	Online training with live interaction between real-world AT agent and synthetic market

2 Preliminaries

Limit order book market. In financial markets, traders (either individuals or automated systems) buy (bid) and sell (ask) financial assets based on the available market information, aiming to make a profit. The buy and sell trades/orders are processed through a matching engine, also known as an *exchange*, that operates under specific rules (typically “first in first out”). The most common orders are market orders and limit orders: Market orders are executed immediately at the prevailing bid or ask price, whereas limit orders set an upper (or

lower) price threshold for a buy (or sell) order, and thus may not be (immediately) executed until there is a matching counterparty. As illustrated in Figure 2, the LOB [Gould et al.,

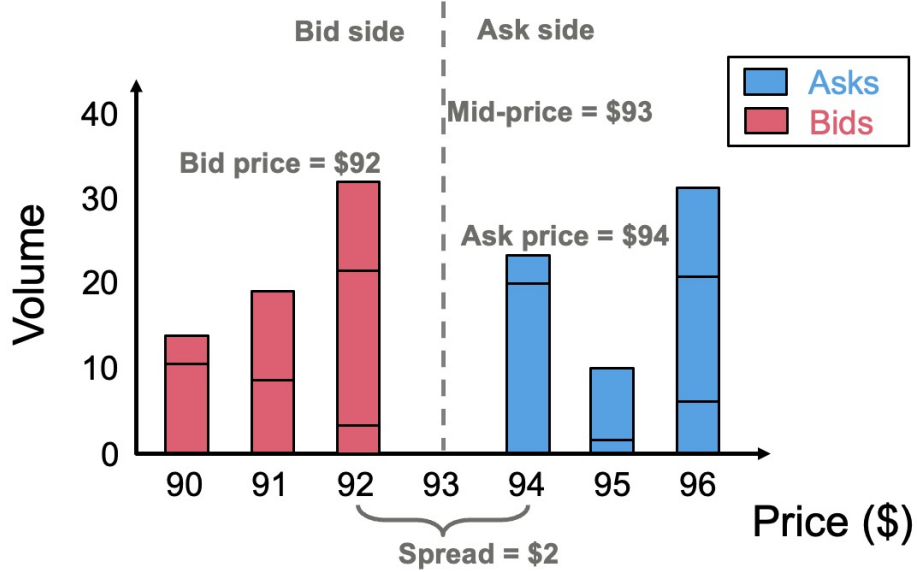


Figure 2: The LOB structure for a specific asset.

2013] organizes and displays outstanding (i.e., unexecuted) limit orders, providing insights into market conditions and liquidity; Its statistical properties, called *stylized facts* [Cont, 2001, Vyetenko et al., 2020], such as mid-price and spread, can help traders with informed decision-making. See Appendix B.1 for more on LOB and stylized facts.

Algorithmic trading under Markov Decision Process formulation. One fundamental problem in financial modeling is algorithmic trading, where an algorithmic agent replaces human traders such that it can analyze large volumes of market data, identify patterns, and execute orders at high speeds; in the meantime, the market responds to the AT agent’s actions in the way that other participants, called *background agents*, adjust their strategies and place orders accordingly. These AT agents can be designed/trained to perform a variety of tasks, e.g., optimal execution, market making, etc. See Appendix B.2 for further details.

We formulate the AT problem as a Markov Decision Process, in which the experimental AT agent interacts with the market to adapt its strategy based on the dynamic feedback from the market. The AT agent can be rule-based, or trained by online reinforcement learning, enabling the agent to make informed decisions sequentially that optimize the trade execution in response to changing market conditions. Formally, denote the state space by \mathcal{S} , action space by \mathcal{A} , and a reward function by R . At each discrete time step $t \in \{1, \dots, T\}$, where T

is a finite time horizon, the experimental AT agent observes the state $s_{t-1} \in \mathcal{S}$, and places an order $a_t \in \mathcal{A}$ according to its policy π ; this action can incur an immediate reward $R(s_{t-1}, a_t)$ and push the market to the next state s_t as the background agents respond to a_t .

Generative model for market simulation. To distinguish between the experimental AT agent and the background world agent, we denote the input to the background world agent as $y \in \mathcal{Y}$, which yields a random action $x \in \mathcal{X}$ through $x = G_\theta(z|y)$, $z \sim N(\mathbf{0}, \mathbf{1})$; Here, G_θ is the neural network parameterized by θ , which implies a conditional distribution on the order placed by the background world agent, i.e.,

$$x \sim p_\theta(\cdot|y). \quad (1)$$

The objective is to train a background world agent to emulate the real background agents, ensuring that the stylized facts of simulated data from the *world agent market*, i.e., the simulated market with the background world agent, closely match reality. Refer to the left panel in Figure 1 for a graphical illustration of the interaction between the AT agent and background agents (i.e., the market).

Data. We use an ordered list \mathcal{T} to denote the collection of states and actions when the AT agent π interacts with the world agent market. We slightly abuse the term *rollout* to denote the collected data during (or after) the interaction between the AT agent and the market. Specifically, the *partial rollout* that ends at time step $t \in \{1, \dots, T\}$ is:

$$\mathcal{T}_{\pi, \theta}^{1:t} = \{s_0, \dots, s_{t-1}, a_t, (y_t^1, x_t^1), \dots, (y_t^{\tau_t}, x_t^{\tau_t})\}.$$

In particular, the prefix that determines the last sequential action, i.e., order $x_t^{\tau_t}$, of the background world agent is

$$\tilde{\mathcal{T}}_{\pi, \theta}^{1:t} = \{s_0, \dots, a_t, (y_t^1, x_t^1), \dots, (y_t^{\tau_t-1}, x_t^{\tau_t-1}), y_t^{\tau_t}\}.$$

3 Methodology

In this section, we will formally define the unique characteristic of the market, which we call a *feedback* f , after the interaction, which we call *rollout*, of a fixed AT agent π with that market. As a result, training market simulators can be done by minimizing the chosen

feedback’s difference between the world agent market and the real market. However, there are two questions to be answered:

- **(Q1)** Which stylized fact can be used as f to characterize the market?
- **(Q2)** Since the evaluation of f after rollout involves operations from the highly non-differentiable exchange, how to minimize the feedback difference between the real market and the world-agent market?

Here, we leave the feedback choice unspecified and answer Q2 by adapting the SeqGAN [Yu et al., 2017] to our problem. In the next section, we will answer Q1 with empirical evidence.

3.1 A distance metric between markets

Feedback f . For AT agent with policy π , the feedback can be obtained through its rollout under world agent (or real) market. Formally, given the complete rollout $\mathcal{T}_{\pi,\theta}^{1:T}$ under world agent market, the feedback is denoted by $f(\mathcal{T}_{\pi,\theta}^{1:T})$, which can be understood as a realization of random variable (r.v.) $f(\pi, p_\theta)$ shown in the right panel of Figure 1, where the randomness comes from the stochastic policy p_θ (1). Similarly, we use subscript **real** to denote the feedback for rollout under real market, i.e., $f(\mathcal{T}_{\pi,\text{real}}^{1:T})$, which can be viewed as a realization of r.v. $f(\pi, p_{\text{real}})$.

Market distance metric D_f . Given f , our proposed market distance metric, which is highlighted in red in Figure 1 and will be used to train the world agent, is defined as:

$$D_f(\theta) = \hat{d} \left(\{f(\mathcal{T}_{i,\pi,\theta}^{1:T}), i = 1, \dots, N\}, \{f(\mathcal{T}_{j,\pi,\text{real}}^{1:T}), j = 1, \dots, N'\} \right), \quad (2)$$

where $\mathcal{T}_{i,\pi,\theta}^{1:T}$ ’s and $\mathcal{T}_{j,\pi,\text{real}}^{1:T}$ ’s are the complete rollouts under the world agent market and real market, respectively. Here, \hat{d} represents an empirical estimate of a distance metric between probability distributions. A popular example is Maximum Mean Discrepancy (MMD) [Gretton et al., 2012]. Please see further details, including a graphical illustration of the evaluation of D_f (see Figure 12) and the expression of an unbiased estimate of MMD in Appendix C.2.

3.2 Market simulator training via D_f

Here, we introduce ATMS, a world agent trained by minimizing our AT-based market distance metric D_f (2). One major technical challenge arises as evaluating D_f involves

non-differentiable operations, such as order deletions from the LOB, during the exchange interaction. Thus, commonly used numerical methods, e.g., back-propagation, for gradient descent (GD) become generally infeasible.

Training objective. To handle the non-differentiable metric issue, one popular approach is SeqGAN, which addresses this challenge by reformulating the generator as a stochastic RL policy and leveraging the Policy Gradient Theorem [Sutton et al., 1999]. Fortunately, our problem formulation aligns with SeqGAN’s in the sense that the world agent generates orders sequentially, and the AT-based metric evaluation occurs only at the end of the rollout (to be discussed in Remark 1). Inspired by SeqGAN, our ATMS is done by:

$$\theta = \arg \min_{\theta} \mathcal{L}(\theta) = \sum_{x \in \mathcal{X}} p_{\theta}(x|y_1^{\tau_1}) Q_f(\tilde{\mathcal{T}}_{\pi, \theta}^{1:1}, x),$$

where the input to world agent $y_1^{\tau_1}$ is the last element in the ordered list $\tilde{\mathcal{T}}_{\theta}^{1:1}$, and Q_f is the state-action value function, i.e., the cumulative expected cost conditional on start state $\tilde{\mathcal{T}}_{\theta}^{1:1}$ and action x following the stochastic policy p_{θ} (1).

Proposed metric as value function. We choose the value function Q_f to be our proposed metric D_f (2) with complete rollouts, assuming all intermediate costs are zeros. To be precise, at the intermediate stage of the rollout (say at t -th step), Q_f can be estimated through N Monte Carlo (MC) simulations to finish the rollout, referred to as MC rollouts:

$$Q_f(\tilde{\mathcal{T}}_{\pi, \theta}^{1:t}, x) = \hat{d}(f(\mathcal{T}_{\pi, \theta}^{\text{MC}}), f(\mathcal{T}_{\pi, \text{real}})),$$

where $f(\mathcal{T}_{\pi, \theta}^{\text{MC}})$ denotes the collection of feedbacks obtained from N MC rollouts with prefix $\tilde{\mathcal{T}}_{\pi, \theta}^{1:t} \cup \{x\}$, i.e.,

$$f(\mathcal{T}_{\pi, \theta}^{\text{MC}}) = \left\{ f(\mathcal{T}_{i, \pi, \theta}^{1:T, \text{MC}}) : \tilde{\mathcal{T}}_{\pi, \theta}^{1:t} \cup \{x\} \subset \mathcal{T}_{i, \pi, \theta}^{1:T, \text{MC}}, \quad i = 1, \dots, N \right\}, \quad (3)$$

and $f(\mathcal{T}_{\pi, \text{real}})$ denotes the collection of feedbacks obtained from N' complete rollouts under the real market, i.e.,

$$f(\mathcal{T}_{\pi, \text{real}}) = \left\{ f(\mathcal{T}_{j, \pi, \text{real}}^{1:T}), \quad j = 1, \dots, N' \right\}. \quad (4)$$

Gradient estimation. The Policy Gradient Theorem gives a closed-form expression of the gradient of the objective function \mathcal{L} with respect to (w.r.t.) generator network parameter θ without differentiating AT-based Q_f , i.e.,

$$\nabla_{\theta} \mathcal{L}(\theta) = \sum_{t=1}^T \mathbb{E}_{\tilde{\mathcal{T}}_{\pi, \theta}^{1:t}} \left[\sum_{x_t \in \mathcal{X}} \nabla_{\theta} p_{\theta}(x_t | y_t^{\tau_t}) \cdot Q_f(\tilde{\mathcal{T}}_{\pi, \theta}^{1:t}, x_t) \right],$$

where $y_t^{\tau_t}$ is the last element of the ordered list $\tilde{\mathcal{T}}_{\pi, \theta}^{1:t}$. Next, the likelihood-ratio technique [Glynn, 1990] is invoked to obtain an unbiased empirical estimate of the gradient, i.e.,

$$\begin{aligned} \nabla_{\theta} \mathcal{L}(\theta) &\simeq \sum_{t=1}^T \sum_{x_t \in \mathcal{X}} \nabla_{\theta} p_{\theta}(x_t | y_t^{\tau_t}) \cdot Q_f(\tilde{\mathcal{T}}_{\pi, \theta}^{1:t}, x_t) \\ &= \sum_{t=1}^T \sum_{x_t \in \mathcal{X}} p_{\theta}(x_t | y_t^{\tau_t}) \nabla_{\theta} \log p_{\theta}(x_t | y_t^{\tau_t}) \cdot Q_f(\tilde{\mathcal{T}}_{\pi, \theta}^{1:t}, x_t) \\ &= \sum_{t=1}^T \mathbb{E}_{x_t \sim p_{\theta}(\cdot | y_t^{\tau_t})} \left[\nabla_{\theta} \log p_{\theta}(x_t | y_t^{\tau_t}) \cdot Q_f(\tilde{\mathcal{T}}_{\pi, \theta}^{1:t}, x_t) \right], \end{aligned}$$

where $\tilde{\mathcal{T}}_{\pi, \theta}^{1:1} \subset \dots \subset \tilde{\mathcal{T}}_{\pi, \theta}^{1:T}$ all come from a complete rollout $\mathcal{T}_{\pi, \theta}^{1:T}$ under world agent market p_{θ} . The expectation in the last line of the above equation can be approximated via sample average.

Here, we present the details for training ATMS with policy gradient update in Algorithm 1. See Appendix C for further details of practical implementation, including a graphical illustration of how to back-propagate to obtain the gradient in Figure 13 in Appendix C.4.

4 Experiments

In this section, we provide numerical evidence to justify our selection of the feedback function f and the probability distance \hat{d} . We use ABIDES with explicitly specified background agents, treated as the “real” market, to train a world agent capable of generating market data with realistic stylized facts. The AT agent performs an optimal execution task, aiming to acquire (or liquidate) a fixed share of a single asset within a fixed time horizon while minimizing the transaction cost (or maximizing the profit). To improve simulator resilience under unseen and rare market states [Coletta et al., 2023], the AT agent places aggressive orders. Its input includes private state (current time and remaining shares) and market state (such as spread). The background world agent takes the market state from the past five steps as input [Coletta

Algorithm 1 Policy gradient update for algorithmic trading-guided market simulation

Input: Real-world AT agent policy π , feedback in reality $f(\mathcal{T}_{\pi, \text{real}})$ (4), empirical probability distance \hat{d} , learning rate r , time horizon T , batch size b , rollout number N .

```
1: while convergence not achieved do
2:   Perform a complete rollout following  $p_\theta$ :  $\mathcal{T}_{\pi, \theta}^{1:T}$ .
3:   for  $t = 1$  to  $T$  do
4:     Given prefix  $\tilde{\mathcal{T}}_\theta^{1:t} = \{\dots, y_t^{\tau_t}\} \subset \mathcal{T}_{\pi, \theta}^{1:T}$ , sample:  $x_{t,1}, \dots, x_{t,b} \sim p_\theta(\cdot | y_t^{\tau_t})$ .
5:     for  $k = 1$  to  $b$  do
6:       Finish  $N$  MC rollouts with prefix  $\tilde{\mathcal{T}}_\theta^{1:t} \cup \{x_{t,k}\}$  following  $p_\theta$ :  $\mathcal{T}_{\pi, \theta}^{\text{MC}}$  (3).
7:       Compute:  $Q_f^{t,k} = \hat{d}(f(\mathcal{T}_{\pi, \theta}^{\text{MC}}), f(\mathcal{T}_{\pi, \text{real}}))$ .
8:     end for
9:   end for
10:   $\theta \leftarrow \theta - r \sum_{t=1}^T \frac{1}{b} \sum_{k=1}^b Q_f^{t,k} \nabla_\theta \log p_\theta(x_{t,k} | y_t^{\tau_t})$ .
11: end while
12: return  $\theta$ 
```

et al., 2022]. See further details in Appendix D.1.

Here, we validate the proposed market distance metric and our ATMS using semi-real market data since it is easier to obtain the “ground truth”; since this work is still in its preliminary stage, neither the method proposed (i.e., our ATMS) nor the AT agent used therein is currently in production. The experiments here are designed to demonstrate the effectiveness of the proposed metric and training scheme of ATMS, which can support the generalization and deployment of them to the real market in the future.

4.1 An AT-based metric to differentiate markets

In the first part, we use numerical evidence to select feedback f and empirical probability distance metric \hat{d} . We start with the most straightforward candidate feedback — the end-of-rollout cumulative reward of the AT agent, denoted by `EpisodeReward` — and plot its empirical distribution under world agent market and real market in Figure 3. We can observe that: for sufficiently large number of rollouts ($N = 100$, the last column in Figure 3), both visual evidence and quantitative metric MMD support `EpisodeReward`’s effectiveness in differentiating markets. However, taking $N = 100$ incurs unreasonably high computational cost — as shown in Algorithm 1, N MC rollouts (step 7) are needed $T \times b$ times for each iteration in ATMS training (see further discussion on complexity in Section 4.3). Given the constraint on N , with a limited number of rollouts, it is difficult to differentiate two different markets, as shown in the first three columns in Figure 3. These observations render

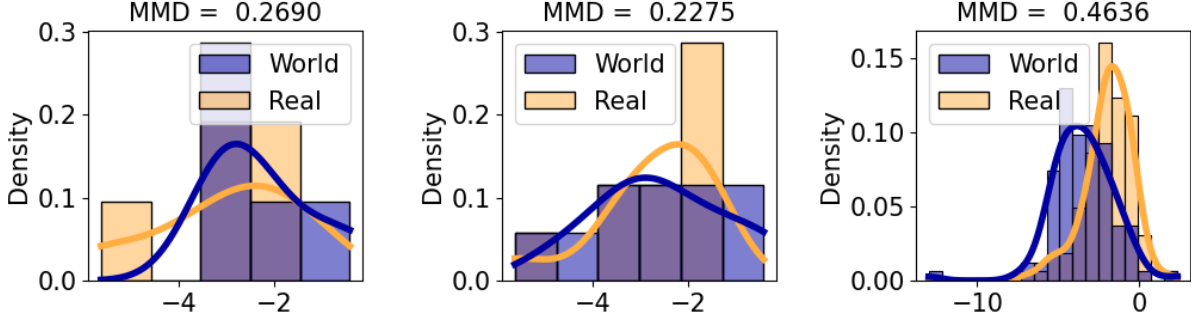


Figure 3: The distribution of `EpisodeReward` under multiple rollouts (from left to right: 5, 10, 100) using AT agent in real (orange) or world agent (blue) markets.

`EpisodeReward` undesirable for training the world agent.

Axioms for ideal candidate feedback. Based on the above analysis, we propose two axioms that f must satisfy:

- (Ax1) Separability — f must be able to differentiate different markets in the sense that f ’s under different markets should be very different;
- (Ax2) Fast convergence — f should have its distribution quickly “converge” to the final state so that only few rollouts are needed during the generator network training.

Indeed, `EpisodeReward` ignores the market dynamics encoded in the time series data collected during the rollout (just as the classic training loss does), and this might explain the observation that the “convergence” w.r.t. number of rollouts is not fast enough, resulting in inefficient data usage and much information loss.

Causal effect from AT agent action to next-step market return as f . Since the main difference between the real market and the world-agent market comes from the background agents, the feedback should depend on those background agents. As illustrated in Figure 1, the effect from AT agent action a_t to next state s_t reflects how background agents respond to a_t , and therefore the resulting feedback can characterize the background agents (and thus the market). To be more precise, we consider the action “placing market order” since market orders are more frequently seen than limit orders; The stylized fact we consider as the next-step state is return, which is the best (in the sense of the aforementioned 2 axioms) compared to other candidates including spread, imbalance, direction and price impact. For brevity, we name this feedback as `Mkt2NextReturn`.

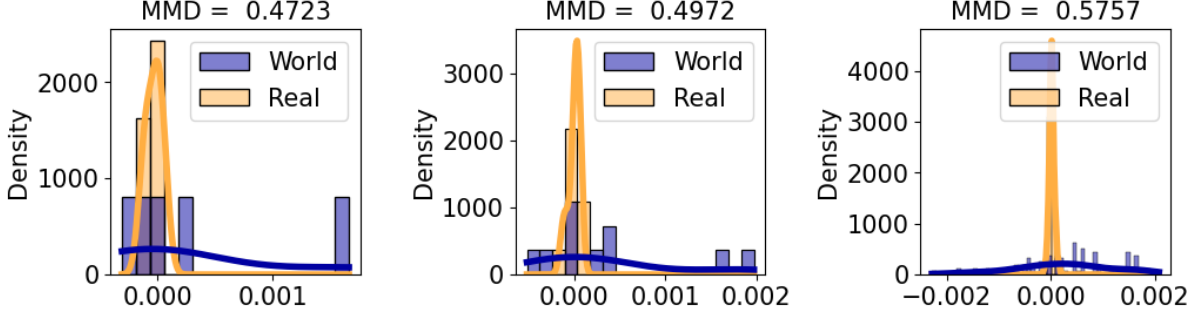


Figure 4: The distribution of `Mkt2NextReturn` under multiple rollouts (from left to right: 5, 10, 100) using AT agent in real (orange) or world agent (blue) markets.

The estimation of `Mkt2NextReturn` can be cast as a causal/treatment effect estimation problem [Rubin, 1974], as s_{t-1} acts as the common cause (or rather, confounder) of both action a_t (i.e., treatment) and next state s_t (i.e., observed outcome). To adjust for confounding, we apply the inverse probability weighted estimator of `Mkt2NextReturn`. In Figure 4, we report the empirical distribution of estimated `Mkt2NextReturn` against increasing rollout number, from which we can observe that with only 5 rollouts the empirical distributions are very different from each other (also verified by MMD) and they are fairly close to the “convergence state” at 100 rollouts. As a result, choosing `Mkt2NextReturn` as f can differentiate two different markets with a small number of rollouts.

To further support our claim and feedback choice above, we consider the effect from action a_t to immediate reward $R(s_{t-1}, a_t)$, denoted by `Mkt2Reward`. Since it is determined by the current LOB status and the exchange rule and does not depend on the background agent, we should expect that it is also a poor candidate. Here, we report the result for `Mkt2Reward` in Figure 5, which exhibits a similar pattern to `EpisodeReward`, providing evidence to support our claim that `Mkt2Reward` solely depends on the current LOB status and the exchange rule, and thus cannot represent the background agents.

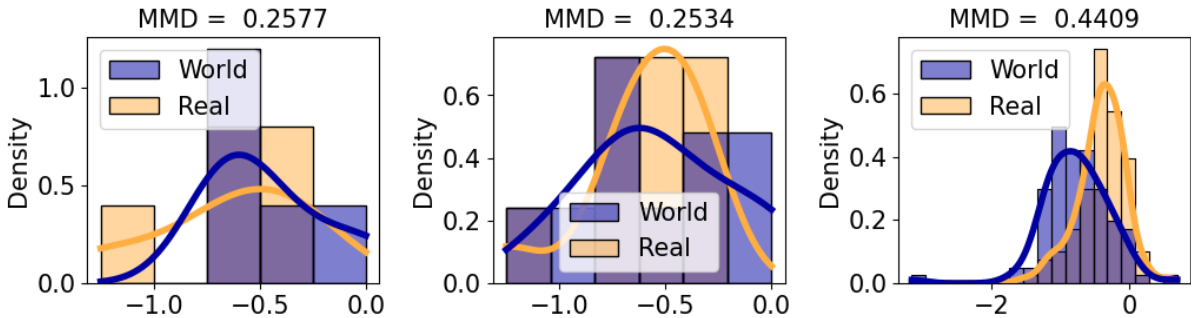


Figure 5: The distribution of `Mkt2Reward` when performing multiple (from left to right: 5, 10, 100) rollouts using AT agent under real (orange) or world agent (blue) markets.

For completeness, we report the results for other stylized facts as the next state in Figure 14 in Appendix D.2, which generally performs worse compared to the return in terms of (Ax1) and (Ax2), suggesting that those stylized facts might be less representative of the market. In particular, we want to mention that Figure 14 shows that using price impact as the next state performs nearly as well as using return. In the next subsection, we will demonstrate that employing `Mkt2NextPriceImpact` as f leads to a closer resemblance of cumulative number of executed profile to reality, while `Mkt2NextReturn` improves the match of volume at first n -levels in the LOB.

MMD as \hat{d} . To train world agent using D_f (2) in the objective function, \hat{d} should also be properly chosen such that D_f meets (Ax1) and (Ax2). To ensure the good separation shown in Figure 4 is not a result of certain random seeds, we perform bootstrap to quantify the uncertainty: For rollout number $N \in \{2, 3, 5, 7, 10, 20, 30, 40, 50\}$, we select N rollouts from 200 rollouts and repeat this procedure 50 times to obtain 50 MMDs; We plot the mean and 5% - 95% envelope, i.e., 90% bootstrap confidence interval (CI), trajectory of those MMDs against N when the two markets are different (or identical) in Figure 6; additionally, we

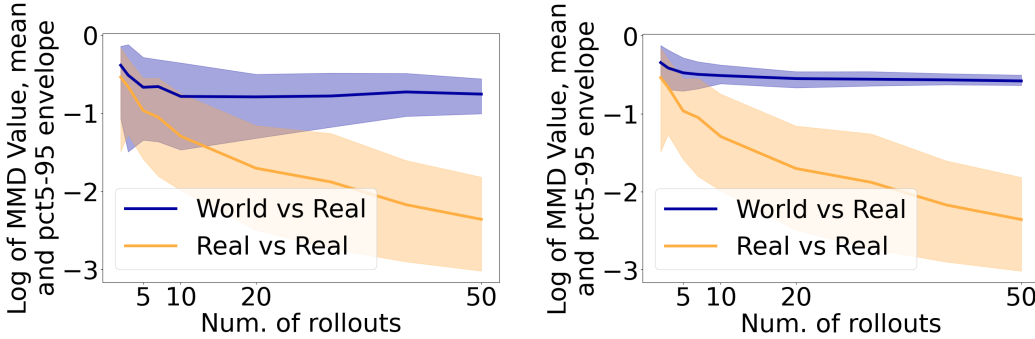


Figure 6: The mean and 90% CI trajectory of proposed loss, with `EpisodeReward` (left) and `Mkt2NextReturn` (right) as f , and empirical MMD as \hat{d} , against increasing number of rollouts.

report result for `EpisodeReward` as f for comparison. We can observe that MMDs under the same market (red) are significantly smaller than that under different markets (blue) when N exceeds 5, verifying D_f 's effectiveness when choosing `Mkt2NextReturn` as f and MMD as \hat{d} to differentiate markets. On the contrary, such a pattern can only be observed for large enough N (around 30) when we consider `EpisodeReward` as f . For completeness, we report the results for ED and EMD in Figure 15 and similar results for other feedback candidates such as `Mkt2NextReward` in Figure 16, and those results reaffirm our choice that `Mkt2NextReturn` as f and MMD as \hat{d} , which will be used later to train the world agent.

Remark 1 (Evaluation at the end of rollout). Indeed, evaluating f as well as D_f using partial rollout (i.e., ignoring step 7 in Algorithm 1) is feasible, but will lead to insufficient rollout time series data for the feedback estimation and metric evaluation. This will result in a metric that fails to differentiate markets and is thus less favorable.

4.2 ATMS: generator training with D_f

Effectiveness of ATMS. We evaluate our ATMS in terms of not only our novel metric, but also visualizing certain stylized facts over time Bouchaud et al. [2018], Li et al. [2020], Vyetrenko et al. [2020]. To demonstrate the effectiveness of our proposed ATMS which minimizes our novel market distance metric, we visualize the stylized fact volume at first

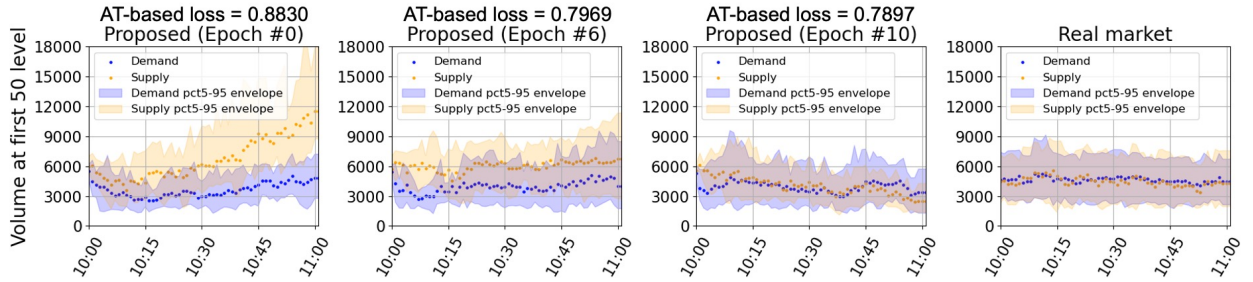


Figure 7: Effectiveness of ATMS. We report volume at first 10-levels. We can observe that the trained generator can generate market data that is increasingly similar to the real market data while minimizing our AT-based metric.

10-levels from 10AM to 11AM over 12 independent trials in Figure 7, from which we can observe that in our proposed ATMS, while the proposed metric is minimized, the stylized fact is “increasingly similar” (in terms of magnitude as well matching demand-supply) to that of the real market.

Comparison with baseline. We show that our ATMS outperforms existing cWGAN baseline [Coletta et al., 2022]; See Appendix B.3 for further details. Interestingly, we find that the stylized facts are not only similar to the target market but also show more balanced BUY and SELL volumes. While the cWGAN training can be biased towards one direction Coletta et al. [2023], our novel approach seems to provide a more fair metric and avoid such biases. Thus we can mitigate the weakness shown in Coletta et al. [2023], where a fairly simple, yet effective, strategy is able to exploit such biases and turn the BUY/SELL unbalance into a profit. Indeed, as illustrated in Figure 1, unlike conventional methods that directly penalize the background world agent’s actions $x_t^{(j)}$ ’s for given inputs $y_t^{(j)}$ ’s, our proposed

ATMS penalizes the AT agent input s_t for given previous step’s AT agent action a_t . As a result, by considering that AT agent input (or state) s contains numerous stylized facts characterizing the market, our approach enables the world agent generator network to produce stylized facts much closer to real markets compared to the cWGAN approach.

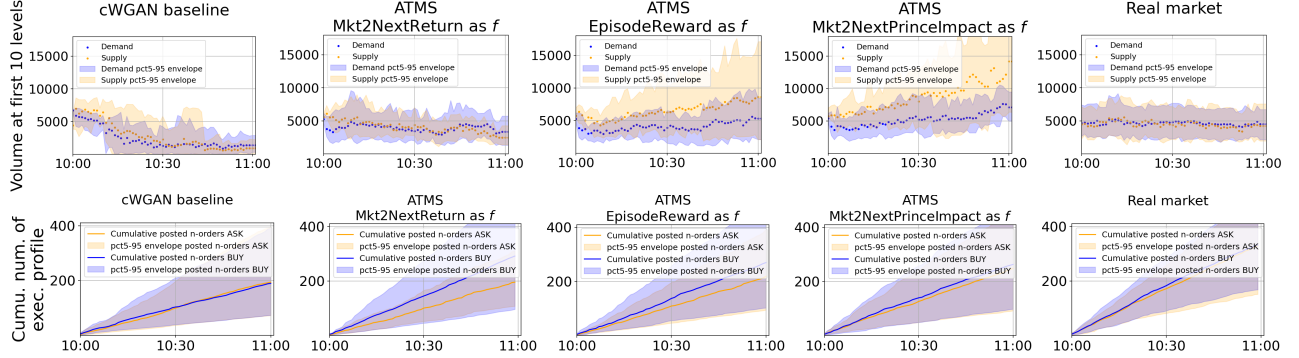


Figure 8: Comparison of volume at first 10-levels between our proposed ATMS and cWGAN baseline. The hyperparameters of training ATMS are specified on top of each panel. The top second column is exactly the third panel in Figure 7, which is the most similar to the real market in terms of supply-demand match and the magnitude.

Specifically, we report our proposed ATMS with different feedback choices in Figure 8. It is interesting to observe that using different f ’s leads to improved similarity to reality for different stylized facts: From the first row of Figure 8, we can see ATMS with *Mkt2NextReturn* as f (second column in the figure) yields volume at first 10-levels most similar to that of real market in the sense that the supply and demand match with each other just like the real market, and their magnitudes are the most more similar to reality; Indeed, using *Mkt2NextReturn* as f in ATMS can lead to the best match of volume at first n -levels in the LOB ($n \in \{1, 5\}$) to the real market as evidenced in Figure 18 in Appendix D.5; Even though ATMS with *Mkt2NextPriceImpact* as f yields very different volume at first 10-levels from reality, it does achieve improved similarity compared to the initialization (see the first panel in Figure 7) in terms of matching supply-demand. From the second row of Figure 8, we can observe that ATMS with *Mkt2NextPriceImpact* as f (fourth column in the figure) can lead to the best cumulative number of executed profile: The improvement compared to *Mkt2NextReturn* is evident, whose BUY is significantly larger than SELL; Compared to cWGAN baseline, it correctly captures not only the magnitudes of SELL and BUY but also the pattern that BUY is slightly larger than SELL. In addition, the third column in Figure 8 serves as “direct evidence” that *EpisodeReward* is not appropriate for training the world agent, reaffirming our previous conclusions.

For completeness, we also show that our proposed ATMS does not lead to performance

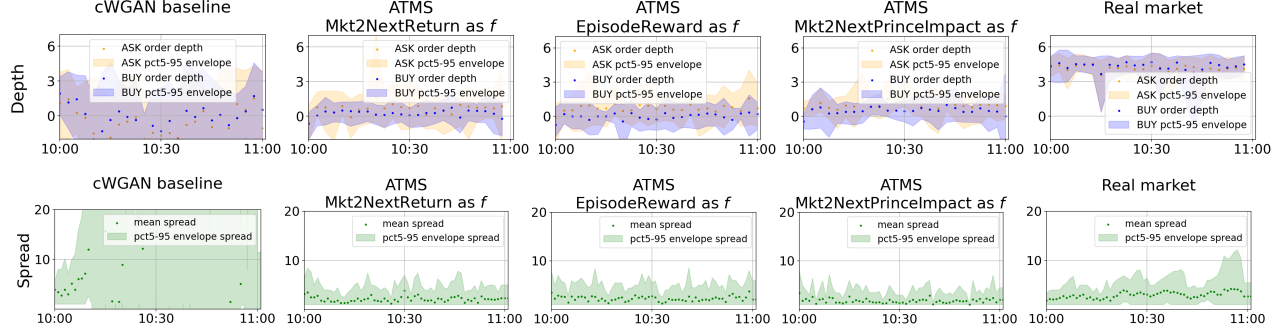


Figure 9: Comparison of additional stylized facts (top: depth; bottom: spread) among different simulated markets (specified on top of each panel). We can observe that our ATMS with various feedback choices can perform a bit better than the cWGAN baseline in terms of the variance of those stylized facts.

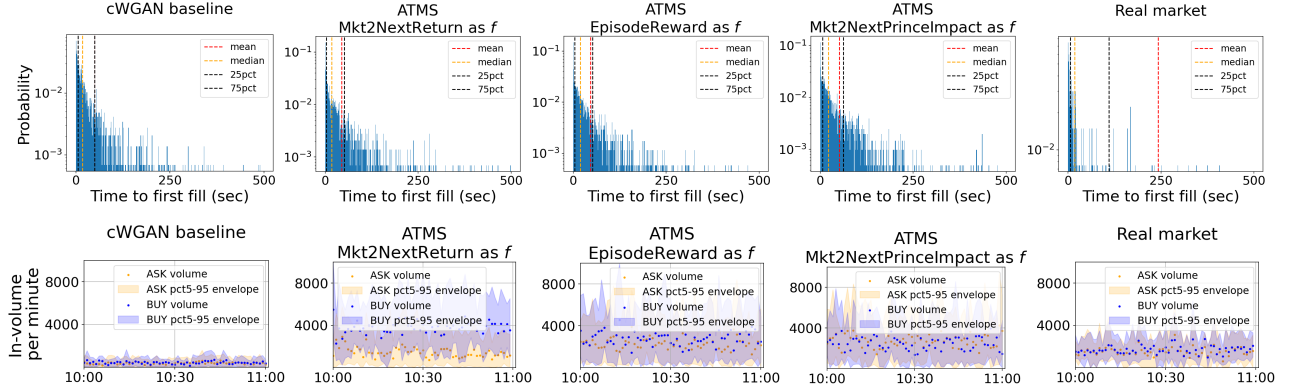


Figure 10: Comparison of additional stylized facts (top: time to first fill; bottom: in-volume per minute) among different simulated markets (specified on top of each panel). We can observe that neither our ATMS nor the cWGAN baseline can correctly capture those stylized facts in real market, suggesting future work to further improve the market simulator.

degradation by exhibiting significantly different behavior from reality in terms of other stylized facts, we present results for those additional stylized facts in Figures 9 and 10. We can observe that there is still a gap between simulated and real markets, and neither our proposed ATMS nor cWGAN can faithfully capture those stylized facts, i.e., generating synthetic market data with those stylized facts similar to reality. Nevertheless, we can observe from Figure 9 that our proposed ATMS have better variance matching to reality compared to the cWGAN baseline for depth and spread, even though all of them do not correctly capture the magnitude. Overall, the above results show that our proposed ATMS with properly chosen feedback can improve the match of certain stylized facts to reality compared to the cWGAN baseline approach.

4.3 Discussion

As illustrated in Figure 1 (and Figure 12 in Appendix C.2), our ATMS only needs a fixed collection of feedbacks under real market $f(\mathcal{T}_{\pi, \text{real}})$ (4), i.e., real market reply, and therefore the deployment of our ATMS does not interfere trading activities under real market. However, the deployment of ATMS does require the AT agent to take real-world strategy, which typically targets very complex financial tasks on a large time horizon T . As a result, one potential limitation is the computational complexity — each iteration (or update of the network parameters) in Algorithm 1 requires $\mathcal{O}(NbT)$ rollouts, resulting in $\mathcal{O}(NbT^2)$ steps in total. Fortunately, our experiment shows that the complexity can be reduced to $\mathcal{O}(NbT_0T)$ by approximating the gradient with

$$\nabla_{\theta} \mathcal{L} \simeq \sum_{t=1}^{T_0} \mathbb{E}_{x \sim p_{\theta}(\cdot | y_t^{\tau_t})} \left[\nabla_{\theta} \log p_{\theta}(x_t | y_t^{\tau_t}) Q_f \left(\tilde{\mathcal{T}}_{\pi, \theta}^{1:t}, x_t \right) \right].$$

Indeed, the effect of b and T_0 in the above gradient estimation determines how many background world agent actions are sampled and penalized (which acts like batch-size in SGD), whereas N controls how well the estimated Q_f is. Our study in Section 4.1 actually tries to find the smallest N to meet Ax2, which guarantees an effective metric, i.e., the estimated Q_f can differentiate simulated and real markets. Then, by carefully tuning b and T_0 (see further details on hyperparameter selection in Appendix D.1), the training of our ATMS can converge within a reasonable time frame (about 2 hours) using Amazon Web Services (r6i.24xlarge, 96 CPUs, 768 GiB memory). As a result, we can properly tune N, b, T_0 , and the complexity will be linear with respect to the horizon T that is determined by the real financial tasks.

5 Conclusion

This work proposes to leverage the downstream task of market simulation — algorithmic trading — to develop a market distance metric, which is used to train the market simulator in return. Our extensive experiments on semi-real market data demonstrate ATMS’s effectiveness in generating more realistic market data compared to the SOTA cWGAN-based simulator. This verifies its generalization to various market data and potential applicability to real-world algorithmic trading strategy construction and testing. An intriguing application of our approach is market change-point detection. By continuously updating the feedback under the real market during the ATMS training, we can capture changes in real market dynamics through the evolution of the trained world agent network parameters. For instance, during the COVID period, training ATMS with continuously updated feedback from the real market could lead to an evolving world agent, based on which we can retrain the trading strategies accordingly. The work in its current state only aims to showcase the effectiveness of our novel metric and training scheme, and we leave further applications of our method as future developments.

Acknowledgment

The authors would like to thank Haibei Zhu for his valuable suggestion on algorithmic trading strategy construction, and Yousef El-Laham for his advice on the method presentation.

Disclaimer

This paper was prepared for informational purposes by the Artificial Intelligence Research group of JPMorgan Chase & Co. and its affiliates (“JP Morgan”), and is not a product of the Research Department of JP Morgan. JP Morgan makes no representation and warranty whatsoever and disclaims all liability, for the completeness, accuracy or reliability of the information contained herein. This document is not intended as investment research or investment advice, or a recommendation, offer or solicitation for the purchase or sale of any security, financial instrument, financial product or service, or to be used in any way for evaluating the merits of participating in any transaction, and shall not constitute a solicitation under any jurisdiction or to any person, if such solicitation under such jurisdiction or to such person would be unlawful.

References

- Robert Almgren and Neil Chriss. Optimal execution of portfolio transactions. *Journal of Risk*, 3:5–40, 2001.
- Selim Amrouni, Aymeric Moulin, Jared Vann, Svitlana Vyetrenko, Tucker Balch, and Manuela Veloso. Abides-gym: gym environments for multi-agent discrete event simulation and application to financial markets. In *Proceedings of the Second ACM International Conference on AI in Finance*, pages 1–9, 2021.
- Martin Arjovsky, Soumith Chintala, and Léon Bottou. Wasserstein generative adversarial networks. In *International conference on machine learning*, pages 214–223. PMLR, 2017.
- Yuntao Bai, Andy Jones, Kamal Ndousse, Amanda Askell, Anna Chen, Nova DasSarma, Dawn Drain, Stanislav Fort, Deep Ganguli, Tom Henighan, et al. Training a helpful and harmless assistant with reinforcement learning from human feedback. *arXiv preprint arXiv:2204.05862*, 2022.
- Tucker Hybinette Balch, Mahmoud Mahfouz, Joshua Lockhart, Maria Hybinette, and David Byrd. How to evaluate trading strategies: Single agent market replay or multiple agent interactive simulation? *arXiv preprint arXiv:1906.12010*, 2019.
- Feryal Behbahani, Kyriacos Shiarlis, Xi Chen, Vitaly Kurin, Sudhanshu Kasewa, Ciprian Stirbu, Joao Gomes, Supratik Paul, Frans A Oliehoek, Joao Messias, et al. Learning from demonstration in the wild. In *2019 International Conference on Robotics and Automation (ICRA)*, pages 775–781. IEEE, 2019.
- Raunak P Bhattacharyya, Derek J Phillips, Changliu Liu, Jayesh K Gupta, Katherine Driggs-Campbell, and Mykel J Kochenderfer. Simulating emergent properties of human driving behavior using multi-agent reward augmented imitation learning. In *2019 International Conference on Robotics and Automation (ICRA)*, pages 789–795. IEEE, 2019.
- Jean-Philippe Bouchaud, Julius Bonart, Jonathan Donier, and Martin Gould. *Trades, quotes and prices: financial markets under the microscope*. Cambridge University Press, 2018.
- David Byrd, Maria Hybinette, and Tucker Hybinette Balch. Abides: Towards high-fidelity multi-agent market simulation. In *Proceedings of the 2020 ACM SIGSIM Conference on Principles of Advanced Discrete Simulation*, pages 11–22, 2020.

- Andrea Coletta, Matteo Prata, Michele Conti, Emanuele Mercanti, Novella Bartolini, Aymeric Moulin, Svitlana Vyetrenko, and Tucker Balch. Towards realistic market simulations: a generative adversarial networks approach. In *Proceedings of the Second ACM International Conference on AI in Finance*, pages 1–9, 2021.
- Andrea Coletta, Aymeric Moulin, Svitlana Vyetrenko, and Tucker Balch. Learning to simulate realistic limit order book markets from data as a world agent. In *Proceedings of the Third ACM International Conference on AI in Finance*, pages 428–436, 2022.
- Andrea Coletta, Joseph Jerome, Rahul Savani, and Svitlana Vyetrenko. Conditional generators for limit order book environments: Explainability, challenges, and robustness. *arXiv preprint arXiv:2306.12806*, 2023.
- Rama Cont. Empirical properties of asset returns: stylized facts and statistical issues. *Quantitative finance*, 1(2):223, 2001.
- Brandon Da Silva and Sylvie Shang Shi. Style transfer with time series: Generating synthetic financial data. *arXiv preprint arXiv:1906.03232*, 2019.
- Chelsea Finn, Paul Christiano, Pieter Abbeel, and Sergey Levine. A connection between generative adversarial networks, inverse reinforcement learning, and energy-based models. *arXiv preprint arXiv:1611.03852*, 2016.
- Justin Fu, Katie Luo, and Sergey Levine. Learning robust rewards with adversarial inverse reinforcement learning. *arXiv preprint arXiv:1710.11248*, 2017.
- Peter W Glynn. Likelihood ratio gradient estimation for stochastic systems. *Communications of the ACM*, 33(10):75–84, 1990.
- Alejandro Gomez-Alanis, Jose A Gonzalez-Lopez, and Antonio M Peinado. A kernel density estimation based loss function and its application to asv-spoofing detection. *IEEE Access*, 8:108530–108543, 2020.
- Ian Goodfellow, Jean Pouget-Abadie, Mehdi Mirza, Bing Xu, David Warde-Farley, Sherjil Ozair, Aaron Courville, and Yoshua Bengio. Generative adversarial nets. *Advances in neural information processing systems*, 27, 2014.
- Martin D Gould, Mason A Porter, Stacy Williams, Mark McDonald, Daniel J Fenn, and Sam D Howison. Limit order books. *Quantitative Finance*, 13(11):1709–1742, 2013.

- Arthur Gretton, Karsten M Borgwardt, Malte J Rasch, Bernhard Schölkopf, and Alexander Smola. A kernel two-sample test. *Journal of Machine Learning Research*, 13(Mar):723–773, 2012.
- Ben Hambly, Renyuan Xu, and Huining Yang. Recent advances in reinforcement learning in finance. *arXiv preprint arXiv:2112.04553*, 2021.
- Jonathan Ho and Stefano Ermon. Generative adversarial imitation learning. *Advances in neural information processing systems*, 29, 2016.
- Daniel G Horvitz and Donovan J Thompson. A generalization of sampling without replacement from a finite universe. *Journal of the American statistical Association*, 47(260):663–685, 1952.
- Abdul Jabbar, Xi Li, and Bourahla Omar. A survey on generative adversarial networks: Variants, applications, and training. *ACM Computing Surveys (CSUR)*, 54(8):1–49, 2021.
- Michaël Karpe, Jin Fang, Zhongyao Ma, and Chen Wang. Multi-agent reinforcement learning in a realistic limit order book market simulation. In *Proceedings of the First ACM International Conference on AI in Finance*, pages 1–7, 2020.
- Adriano Koshiyama, Nick Firoozye, and Philip Treleaven. Generative adversarial networks for financial trading strategies fine-tuning and combination. *Quantitative Finance*, 21(5): 797–813, 2021.
- Ashutosh Kumar, Arijit Biswas, and Subhajit Sanyal. ecommercegan: A generative adversarial network for e-commerce. *arXiv preprint arXiv:1801.03244*, 2018.
- Chia-Hsuan Kuo, Chiao-Ting Chen, Sin-Jing Lin, and Szu-Hao Huang. Improving generalization in reinforcement learning-based trading by using a generative adversarial market model. *IEEE Access*, 9:50738–50754, 2021.
- Junyi Li, Xintong Wang, Yaoyang Lin, Arunesh Sinha, and Michael Wellman. Generating realistic stock market order streams. In *Proceedings of the AAAI Conference on Artificial Intelligence*, volume 34, pages 727–734, 2020.
- Charles M Macal and Michael J North. Tutorial on agent-based modeling and simulation. In *Proceedings of the Winter Simulation Conference, 2005.*, pages 14–pp. IEEE, 2005.

- Mehdi Mirza and Simon Osindero. Conditional generative adversarial nets. *arXiv preprint arXiv:1411.1784*, 2014.
- Volodymyr Mnih, Koray Kavukcuoglu, David Silver, Alex Graves, Ioannis Antonoglou, Daan Wierstra, and Martin Riedmiller. Playing atari with deep reinforcement learning. *arXiv preprint arXiv:1312.5602*, 2013.
- Yuriy Nevmyvaka, Yi Feng, and Michael Kearns. Reinforcement learning for optimized trade execution. In *Proceedings of the 23rd international conference on Machine learning*, pages 673–680, 2006.
- Zhaoqing Pan, Weijie Yu, Xiaokai Yi, Asifullah Khan, Feng Yuan, and Yuhui Zheng. Recent progress on generative adversarial networks (gans): A survey. *IEEE access*, 7:36322–36333, 2019.
- Robert Pardo. *The evaluation and optimization of trading strategies*, volume 314. John Wiley & Sons, 2011.
- Yagna Patel. Optimizing market making using multi-agent reinforcement learning. *arXiv preprint arXiv:1812.10252*, 2018.
- Michael Quinlan, Tsz-Chiu Au, Jesse Zhu, Nicolae Stiuca, and Peter Stone. Bringing simulation to life: A mixed reality autonomous intersection. In *2010 IEEE/RSJ International Conference on Intelligent Robots and Systems*, pages 6083–6088. IEEE, 2010.
- Donald B Rubin. Estimating causal effects of treatments in randomized and nonrandomized studies. *Journal of educational Psychology*, 66(5):688, 1974.
- Nataniel Ruiz, Samuel Schuler, and Manmohan Chandraker. Learning to simulate. In *International Conference on Learning Representations*, 2019.
- Muhammad Sarmad, Hyunjoon Jenny Lee, and Young Min Kim. Rl-gan-net: A reinforcement learning agent controlled gan network for real-time point cloud shape completion. In *Proceedings of the IEEE/CVF Conference on Computer Vision and Pattern Recognition*, pages 5898–5907, 2019.
- Jürgen Schmidhuber. On learning to think: Algorithmic information theory for novel combinations of reinforcement learning controllers and recurrent neural world models. *arXiv preprint arXiv:1511.09249*, 2015.

- Dino Sejdinovic, Bharath Sriperumbudur, Arthur Gretton, and Kenji Fukumizu. Equivalence of distance-based and rkhs-based statistics in hypothesis testing. *The annals of statistics*, pages 2263–2291, 2013.
- Jing-Cheng Shi, Yang Yu, Qing Da, Shi-Yong Chen, and An-Xiang Zeng. Virtual-taobao: Virtualizing real-world online retail environment for reinforcement learning. In *Proceedings of the AAAI Conference on Artificial Intelligence*, volume 33, pages 4902–4909, 2019.
- Zijian Shi and John Cartlidge. Neural stochastic agent-based limit order book simulation: A hybrid methodology. In *Proceedings of the 2023 International Conference on Autonomous Agents and Multiagent Systems*, pages 2481–2483, 2023.
- Kihyuk Sohn, Honglak Lee, and Xinchen Yan. Learning structured output representation using deep conditional generative models. *Advances in neural information processing systems*, 28, 2015.
- Victor Storch, Svitlana Vyetrenko, and Tucker Balch. Learning who is in the market from time series: market participant discovery through adversarial calibration of multi-agent simulators. *arXiv preprint arXiv:2108.00664*, 2021.
- Simon Suo, Sebastian Regalado, Sergio Casas, and Raquel Urtasun. Trafficsim: Learning to simulate realistic multi-agent behaviors. In *Proceedings of the IEEE/CVF Conference on Computer Vision and Pattern Recognition*, pages 10400–10409, 2021.
- Richard S Sutton and Andrew G Barto. *Reinforcement learning: An introduction*. MIT press, 2018.
- Richard S Sutton, David McAllester, Satinder Singh, and Yishay Mansour. Policy gradient methods for reinforcement learning with function approximation. *Advances in neural information processing systems*, 12, 1999.
- Yuan Tian, Qin Wang, Zhiwu Huang, Wen Li, Dengxin Dai, Minghao Yang, Jun Wang, and Olga Fink. Off-policy reinforcement learning for efficient and effective gan architecture search. In *Computer Vision–ECCV 2020: 16th European Conference, Glasgow, UK, August 23–28, 2020, Proceedings, Part VII 16*, pages 175–192. Springer, 2020.
- Faraz Torabi, Garrett Warnell, and Peter Stone. Generative adversarial imitation from observation. *arXiv preprint arXiv:1807.06158*, 2018.

- Faraz Torabi, Garrett Warnell, and Peter Stone. Recent advances in imitation learning from observation. *arXiv preprint arXiv:1905.13566*, 2019.
- Svitlana Vyetrenko, David Byrd, Nick Petosa, Mahmoud Mahfouz, Danial Dervovic, Manuela Veloso, and Tucker Balch. Get real: Realism metrics for robust limit order book market simulations. In *Proceedings of the First ACM International Conference on AI in Finance*, pages 1–8, 2020.
- Magnus Wiese, Robert Knobloch, Ralf Korn, and Peter Kretschmer. Quant gans: deep generation of financial time series. *Quantitative Finance*, 20(9):1419–1440, 2020.
- Shuai Xiao, Mehrdad Farajtabar, Xiaojing Ye, Junchi Yan, Le Song, and Hongyuan Zha. Wasserstein learning of deep generative point process models. *Advances in neural information processing systems*, 30, 2017.
- Shuai Xiao, Hongteng Xu, Junchi Yan, Mehrdad Farajtabar, Xiaokang Yang, Le Song, and Hongyuan Zha. Learning conditional generative models for temporal point processes. In *Proceedings of the AAAI Conference on Artificial Intelligence*, volume 32, 2018.
- Lantao Yu, Weinan Zhang, Jun Wang, and Yong Yu. Seqgan: Sequence generative adversarial nets with policy gradient. In *Proceedings of the AAAI conference on artificial intelligence*, volume 31, 2017.
- Kang Zhang, Guoqiang Zhong, Junyu Dong, Shengke Wang, and Yong Wang. Stock market prediction based on generative adversarial network. *Procedia computer science*, 147:400–406, 2019.
- Yizhe Zhang, Zhe Gan, Kai Fan, Zhi Chen, Ricardo Henao, Dinghan Shen, and Lawrence Carin. Adversarial feature matching for text generation. In *International conference on machine learning*, pages 4006–4015. PMLR, 2017.

Appendix of ATMS: Algorithmic Trading-Guided Market Simulation

Table of Contents

A	Extended Literature Survey	28
B	Additional Background Knowledge	29
B.1	Limit order book	29
B.2	Optimal execution and reinforcement learning	31
B.3	Baseline Market Simulator: Conditional Wasserstein GAN	32
C	Additional Implementation Details of ATMS	33
C.1	Causal effect estimation for feedback	33
C.2	Value function evaluation	34
C.3	Density estimation	36
C.4	Training algorithm	36
D	Additional Experimental Details	36
D.1	Training details	36
D.2	Additional results for other feedback candidates	38
D.3	Additional results for other \hat{d} candidates	38
D.4	Additional evidence for the effectiveness of ATMS	41
D.5	Additional comparison results of other stylized facts	41

A Extended Literature Survey

Reinforcement learning (RL) and generative models, although traditionally considered separate fields, have recently revealed promising connections. One notable application involves leveraging generative models in RL training, particularly relevant in the context of optimal execution tasks in financial markets. Indeed, it is a popular approach to study financial tasks with an interactive simulator: For example, [Karpe et al. \[2020\]](#) trained RL agent to perform optimal execution tasks by interacting with parametric market simulator ABIDES [[Byrd et al., 2020](#), [Amrouni et al., 2021](#)] such that the training process captures real-world dynamics, enabling agents to grasp the consequences of their actions on the responses of other market participants; [Kuo et al. \[2021\]](#), [Koshiyama et al. \[2021\]](#) trained agents to perform downstream financial tasks with the help of a conditional GAN-based market simulator.

One notable work studying the connection between GAN and RL is [Ho and Ermon \[2016\]](#), which proposed to mimic the expert policy from instances by inverse RL (IRL) followed by RL; They theoretically proved that explicitly learning of the cost function in the IRL could be bypassed, which enabled end-to-end learning of the policy from the expert policy instances; Moreover, the resulting imitation learning problem takes a GAN formulation, bridging RL and GAN from a very novel perspective. On one hand, as pointed out by [Yu et al. \[2017\]](#), [Shi et al. \[2019\]](#) as well as our work, the generator can be formulated as the (RL) agent policy, and therefore imitation learning can be used for market simulation, which opens up more possibility in this area (i.e., market simulation). However, it is difficult to train adversarial imitation learning models in practice since careful reward augmentation [[Bhattacharyya et al., 2019](#)] and curriculum design [[Behbahani et al., 2019](#)] are needed in practice, and this might explain why GAN is still the most popular approach for market simulation. We refer readers to [Torabi et al. \[2019\]](#) for a recent survey on imitation learning. On the other hand, as most GAN-based simulators, [Ho and Ermon \[2016\]](#) also used the classic loss function and this is the key difference from our work: the proposed novel AT-based market distance metric and the derived training scheme of ATMS are the main contribution of our work.

Another seemingly closely related work in this direction is [Ruiz et al. \[2019\]](#), who studied the classification problem in the presence of limited real data via a classifier trained on generative models. They claimed to leverage RL to help with the GAN training; However, as pointed out by the reviewer, even though the feedback from evaluating the classifier on the real data can help improve the generative model, there is no clear state and action space definition nor sequential decision-making, rendering the claim of reformulating the GAN training as RL is less convincing. Additionally, other contributions in this direction include

Finn et al. [2016], Fu et al. [2017], who formulated IRL as GAN problem, Sarmad et al. [2019], who proposed to use RL to control the input to generators in the GAN, and Tian et al. [2020], who proposed to use RL to help search for the optimal GAN architecture. However, none of those works leverage RL to develop a metric for the training of the generative model, which is the key difference between our work and those existing works.

B Additional Background Knowledge

B.1 Limit order book

LOB dynamics. We begin with introducing the dynamics of LOB, as shown in Figure 11. Here we illustrate this dynamics of the LOB with three cases:

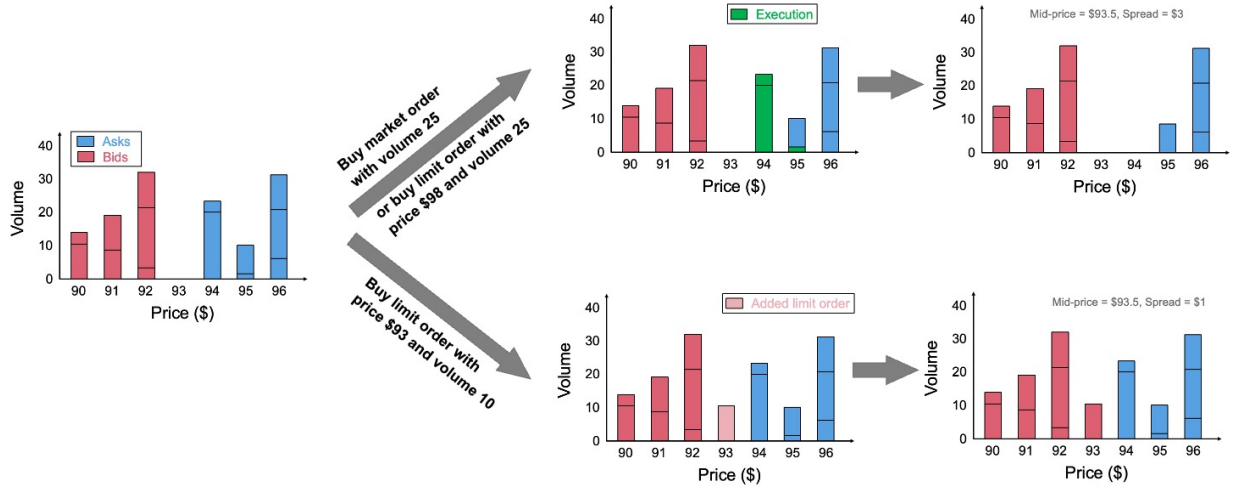


Figure 11: Illustration of the dynamics of LOB.

- Case 1: A buy market order with volume 25 arrives, leading to 25 shares of order executed on ask side based on price and order arrive time. The execution price will be the ask price, and the resulting LOB market will have mid-price and spread shifted to \$93.5 and \$3.
- Case 2: A buy limit order with price \$98 and volume 25 arrives. As \$98 exceeds the current ask price (i.e., \$94), the incoming will be executed at the ask price. The resulting LOB market will be exactly the same with case 1.

- Case 3: A but limit order with price \$93 and volume 10 arrives. Since there will be no matching counterparty on the ask side, this order will be placed in LOB, resulting in LOB market mid-price and spread shift to \$93.5 and \$1.

Stylized facts. Next, we define stylized facts used in this work following the notation in [Coletta et al. \[2022\]](#). We denote $p_a^i(t), v_a^i(t), p_b^i(t), v_b^i(t)$ as the price and volume at i -th level of the LOB, at time t , for ask and bid respectively. For example, in the starting state of the LOB (left panel) shown in Figure 11, $p_a^1(t) = \$94$ and $p_b^1(t) = \$92$. The depth of a limit order with price threshold $p(t)$ is defined as

$$d(t) = \begin{cases} p_b^1(t) - p(t), & \text{If side} = \text{bid}, \\ p_a^1(t) + p(t), & \text{otherwise.} \end{cases}$$

The stylized facts used here are:

- Mid-price, average of ask price and bid price, i.e.,

$$m(t) = \frac{p_a^1(t) + p_b^1(t)}{2}.$$

- Return:

$$r(t) = \log \frac{m(t)}{m(t-1)}.$$

- Spread:

$$\delta(t) = p_a^1(t) - p_b^1(t).$$

- Volume imbalance, the demand and supply inequality within the first n -levels, i.e.,

$$I^n(t) = \frac{\sum_{j=1}^n v_b^j(t)}{\sum_{j=1}^n v_b^j(t) + v_a^j(t)}. \quad (5)$$

- Absolute volume within the first n -levels:

$$V^n(t) = \sum_{j=1}^n v_b^j(t) + v_a^j(t).$$

In particular, the bid (or buy) and ask (or sell) volumes within the first n -levels are

defined as

$$V_b^n(t) = \sum_{j=1}^n v_b^j(t), \quad V_a^n(t) = \sum_{j=1}^n v_a^j(t). \quad (6)$$

B.2 Optimal execution and reinforcement learning

A brief literature survey. One most famous frameworks for optimal execution (or optimized trade execution), where the goal is to sell a target share of stocks within a finite time horizon, would be the Almgren–Chriss Model [Almgren and Chriss, 2001], where the market dynamics takes a parametric form, leading to a “pre-planned strategy that does not depend on real-time market conditions” [Hambly et al., 2021]. To address this issue, Nevmyvaka et al. [2006] first applied RL in the optimal execution problem; However, their RL training used (historic) real data, in which there will be no responses from other traders. [Karpe et al., 2020] leveraged the parametric market simulator ABIDES [Byrd et al., 2020, Amrouni et al., 2021] to generate training data to address this issue. On the contrary, Patel [2018] did consider multiple agents in the RL. For recent advancements in this direction, we refer readers to a nice survey by Hambly et al. [2021] (see Section 4.2 therein).

Reinforcement learning for optimal execution. In the aforementioned optimal execution task, e.g., acquiring q_0 shares of one particular asset within T , the objective function of finding the optimal policy π^* via online RL problem is:

$$\pi^* = \arg \max_{\pi} \mathbb{E}_{\pi} \left[\sum_{t=1}^T \gamma^{t-1} R(s_{t-1}, a_t) - P q_T \right],$$

where $\gamma \in [0, 1]$ is the discount factor that determines the importance of future rewards, \mathbb{E}_{π} denotes the expectation over trajectories generated by policy π , $q_T \geq 0$ denotes amount of unfulfilled shares to meet the target q_0 at the end of rollout, and $P > 0$ is the penalty per unfulfilled share.

Rule-based policy, such as aggressively placing q_0 market orders at the first step, is feasible, but will greatly impact the market and result in sub-optimal profit; Indeed, interacting with the market by executing orders will change the market dynamics, and therefore executing (small) orders sequentially according to the currently observed state is a more sensible strategy.

Deep Q-Network. One popular approach to find the optimal policy for optimal execution is to optimize the action-value function, i.e., the Q-function, which represents the expected cumulative discounted reward starting from state s , taking action a , and following a particular

policy. The optimal Q-function, defined as $\tilde{Q}^*(s, a) = \max_{\pi} \mathbb{E}_{\pi}[\sum_{k=t}^T \gamma^{k-t} R(s_{k-1}, a_k) | s = s_t, a = a_t]$, obeys the Bellman equation:

$$\tilde{Q}^*(s, a) = \mathbb{E}_{\pi} \left[R(s, a) + \gamma \max_{a' \in \mathcal{A}} \tilde{Q}^*(s', a') | s, a \right],$$

where a' is the next-state after agent takes action a at state s . When the state and action spaces are discrete, one can estimate the optimal Q-function by iteratively updating the Q-values as follows:

$$\tilde{Q}_{i+1}(s, a) \leftarrow \tilde{Q}_i(s, a) + \alpha \left(R(s, a) + \gamma \max_{a' \in \mathcal{A}} \tilde{Q}_i(s', a') - \tilde{Q}_i(s, a) \right),$$

where α is the learning rate that controls the weight given to new information. According to [Sutton and Barto \[2018\]](#), this value iteration algorithm converges to the optimal solution, i.e., $\tilde{Q}_i(s, a) \rightarrow \tilde{Q}^*(s, a)$ as $i \rightarrow \infty$. In practice, especially when dealing with high-dimensional or continuous state spaces, the Q-function is often approximated using a Deep Q-Network (DQN), i.e., $\tilde{Q}(s, a; \tilde{\theta}) \approx \tilde{Q}^*(s, a)$, where a deep neural network parameterized by parameter $\tilde{\theta}$ is used to represent the Q-function, enabling generalization to unseen states [[Mnih et al., 2013](#)]. The DQN is trained by minimizing the following objective function (typically via gradient-based method):

$$\tilde{\mathcal{L}}(\tilde{\theta}) = \mathbb{E} \left[\left(R(s, a) + \gamma \max_{a' \in \mathcal{A}} \tilde{Q}(s', a'; \tilde{\theta}) - \tilde{Q}(s, a; \tilde{\theta}) \right)^2 \right].$$

B.3 Baseline Market Simulator: Conditional Wasserstein GAN

Despite the success of variational auto encoder (VAE) [[Sohn et al., 2015](#)] under many other contexts, the most popular machine learning approach for generating market data is still GAN. Conditional GAN (cGAN) [[Mirza and Osindero, 2014](#)] extends the standard GAN [[Goodfellow et al., 2014](#)] framework by incorporating conditional information. The generator network, which acts like a trading agent, G_{θ} takes random noise input z and a conditional variable y to produce synthetic orders x (i.e., random sample z is generated from a prior distribution, such as Gaussian distribution, and then transformed by G_{θ} to “match” the true distribution). The discriminator network D estimates the probability that an order is real by considering both the generated order $G_{\theta}(z|y)$ and the true order x along with the corresponding conditional variable y . The training of a cGAN involves optimizing a min-max

objective function:

$$\min_{\theta} \max_D \mathbb{E}_{x|y \sim p_{\text{real}}, y \sim p_y} [\log D(x|y)] + \mathbb{E}_{z \sim p_z, y \sim p_y} [\log(1 - D(G_{\theta}(z|y)))],$$

where p_{real} represents the real data distribution, p_y represents the distribution of the conditional variable, and p_z represents the prior noise distribution, and y represents the feature/input that cGAN will condition on.

Even though there have been modern machine learning techniques adapted to generative models under various specific domains, such as imitation learning for traffic simulation to test self-driving algorithms [Suo et al., 2021], such adaption for LOB stock market simulation is largely missing until Li et al. [2020], Coletta et al. [2021, 2022], who leveraged cWGANs to train a neural network-based background world agent that places realistic orders based on relevant market information. By utilizing a cWGAN, the world agent can learn from the simulated market data, improving its trading strategies in response to the dynamic market. In particular, Coletta et al. [2021] used Wasserstein distance as the discriminator, i.e., they adopted Wasserstein GAN [Arjovsky et al., 2017]:

$$\min_{\theta} \max_{w \in \mathcal{W}} \mathbb{E}_{x \sim p_{\text{real}}} [f_w(x|y)] - \mathbb{E}_{z \sim p_z} [f_w(G_{\theta}(z|y))],$$

where f_w is the discriminator and the function G_{θ} is the generator. They used gradient descent w.r.t. w and θ iteratively to optimize the objective. Additionally, there exist methods to calibrate ABIDES with advanced machine learning techniques such as GAN [Storchan et al., 2021, Shi and Cartlidge, 2023], the mainstream market simulator is still based on GAN due to its superior performance.

C Additional Implementation Details of ATMS

C.1 Causal effect estimation for feedback

Under the potential outcome framework by Rubin [1974], the causal effect estimation from treatment variable to outcome variable needs to take into account the effect of pre-treatment covariates, called potential confounders. To see why considering the effect from pre-treatment covariates is necessary, let us consider a simple yet popular illustrative example would be studying the effect of carrying a lighter to developing lung cancer: If the effect from smoking, which acts as a common cause to both carrying a lighter and developing lung cancer, is not

considered, a false causal conclusion (which is indeed just correlation) that carrying a lighter will result in lung cancer will be made.

One common approach is to leverage inverse probability weighted (IPW) estimator [Horvitz and Thompson, 1952] to adjust for the potential confounders. In our problem setup, we denote the propensity score, which is the probability of “receiving treatment”, as

$$e(s) = \mathbb{P}(a = \text{placing market order} \mid \text{state} = s) = \pi(s, a),$$

where π is the policy of the AT agent. The IPW estimator of feedback f , i.e., the causal effect from AT agent action to next state, say j -th element of the state vector, is the defined as

$$\frac{1}{T} \sum_{t=1}^T \frac{s_t(j) \mathbf{1}_{\{a_t = \text{placing market order}\}}}{\hat{e}(s_{t-1})},$$

where $s_t(j)$ is the j -th element of the state vector (e.g., return), \hat{e} denotes the estimated propensity score (typically through logistic regression), and $\mathbf{1}$ is the indicator function. In practice, to ensure estimates \hat{e} ’s are not overly small, they are typically clipped using a certain threshold (denoted by PSthres), i.e., $\hat{e} \leftarrow \max\{\hat{e}, \text{PSthres}\}$.

C.2 Value function evaluation

The value function Q_f estimation relies on N' feedbacks from the real market and N feedbacks obtained by performing N complete rollouts under the world agent market. As illustrated in

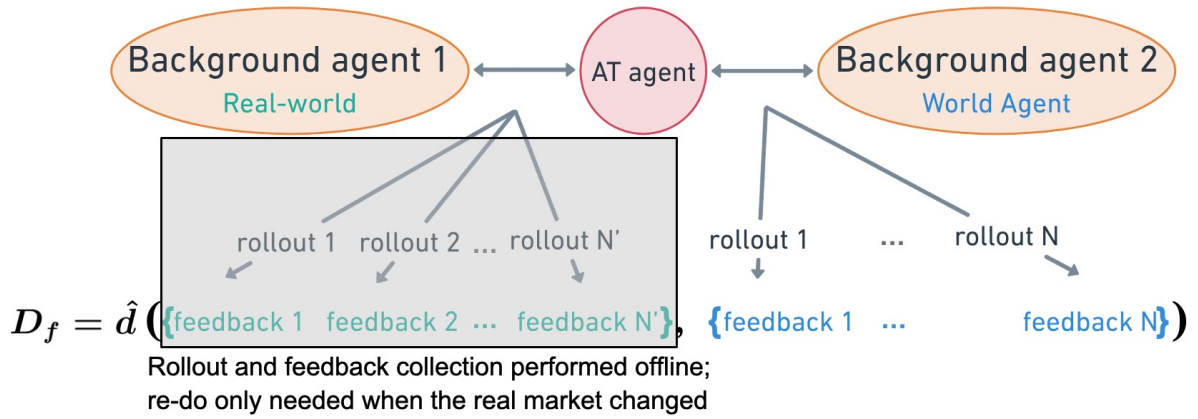


Figure 12: Illustration of the calculation of our proposed AT-based market distance metric.

Figure 12, the rollout under real market to obtain the feedback only needs to be performed offline; during the training of the background world agent generator network (i.e., Algorithm 1),

the rollout under world agent market and the network parameter update are performed iteratively.

In this work, the probability distribution distance metrics we consider are MMD, ED, and EMD. Other discrepancy metrics such as Kullback–Leibler divergence and Jensen–Shannon divergence are less favorable as we can observe the supports of two empirical probability distributions are different in Figures 3, 4, 5 and 14 (especially when the number of rollouts is small).

Given two sets of samples $\{f_1, \dots, f_N\}$ and $\{g_1, \dots, g_{N'}\}$, an unbiased estimator of MMD can be obtained through the following U-statistic [Gretton et al., 2012]:

$$\begin{aligned} \hat{d}_{\text{MMD}}(\{f_1, \dots, f_N\}, \{g_1, \dots, g_{N'}\}) = & \frac{1}{N(N-1)} \sum_{i=1}^N \sum_{j \neq i}^N k(f_i, f_j) - \frac{2}{NN'} \sum_{i=1}^N \sum_{j=1}^{N'} k(f_i, g_j) \\ & + \frac{1}{N'(N'-1)} \sum_{i=1}^{N'} \sum_{j \neq i}^{N'} k(g_i, g_j), \end{aligned}$$

where $k(\cdot, \cdot)$ is the user-specified kernel function. Popular choices include Gaussian kernel with bandwidth parameter $\sigma > 0$,

$$k(f_1, g_1) = \exp\{\|f_1 - g_1\|_2^2 / (2\sigma^2)\},$$

where $\|f_1 - g_1\|_2$ represents the Euclidean distance.

In addition, the empirical estimate of Energy Distance is as follows:

$$\begin{aligned} \hat{d}_{\text{ED}}(\{f_1, \dots, f_N\}, \{g_1, \dots, g_{N'}\}) = & \frac{1}{N(N-1)} \sum_{i=1}^N \sum_{j \neq i}^N \|f_i - f_j\|_2^2 - \frac{2}{NN'} \sum_{i=1}^N \sum_{j=1}^{N'} \|f_i - g_j\|_2^2 \\ & + \frac{1}{N'(N'-1)} \sum_{i=1}^{N'} \sum_{j \neq i}^{N'} \|g_i - g_j\|_2^2. \end{aligned}$$

It is worthwhile noting that ED is a special case of MMD with linear kernel; Indeed, their equivalence has already been established [Sejdinovic et al., 2013]. We do not give further details on the estimation of Earth Mover’s Distance since it is a bit more complex; fortunately, there is built-in implementation of its estimation in `wasserstein_distance` in `scipy.stats`; moreover, later we will use empirical evidence to show that EMD is a less favorable \hat{d} choice.

C.3 Density estimation

Here, since the generator network is a deterministic transformation G_θ , we apply kernel density estimation (KDE) to obtain p_θ since KDE enjoys closed-form and differentiable solutions. In our experiment, we choose a Gaussian RBF kernel with a bandwidth parameter selected using the median heuristic (which is referred to as adaptive bandwidth). Note that using KDE in the objective function is neither novel in literature — there exists work that proposed to include the bandwidth as a model parameter during the optimization [Gomez-Alanis et al., 2020], which is referred to as optimized bandwidth — nor the only approach (i.e., one can choose other density estimation approaches as long as the computational costs are low, or even directly parameterize the density directly with NNs). Additionally, even under our formulation using KDE, there are alternative bandwidth choices, such as fixed bandwidth parameters. Since the bandwidth choice is not a major contribution of this work, we leave the performance of ATM w.r.t. the bandwidth choice as future development, and the user can freely choose among the aforementioned options during the implementation.

C.4 Training algorithm

In this part, we use graphical illustration to show how to perform Algorithmic 1 in practice. In particular, we show the forward pass and back-propagation to obtain the gradient.

D Additional Experimental Details

D.1 Training details

Configuration. In our experiment, the configuration of the optimal execution task is time horizon $T = 10$, parent order size $q_0 = 50$. For the AT agent performing this task, the private state at time step t for the AT agent is normalized elapsed time t/T , remaining shares to acquire normalized by total parent order size q_0 , and their difference; The market state consists of imbalance (i.e., Eq. (5) with all levels and $n = 5$), spread, price impact, and direction feature. The action space $\mathcal{A} = \{0, 1, 2\}$, where action #0 stands for executing fixed size (10 shares in our experiment) Market Order, action #1 stands for executing fixed size Limit Order, and action #2 stands for action hold (i.e., no action). In our experiments on the semi-real market, the external agent places orders aggressively such that the world agent is able to encounter diverse market states. Additionally, this eases the implementation burden as rollout using this simple rule-based AT agent (instead of a neural network-based agent)

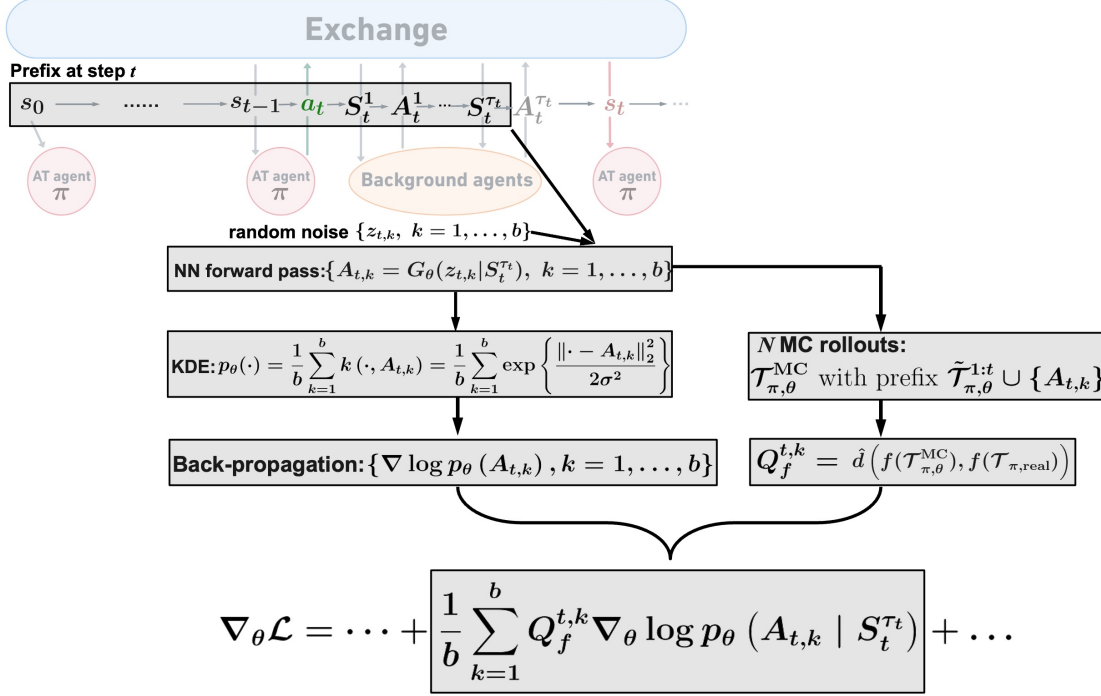


Figure 13: Illustration of Algorithm 1 — the forward-backward pass and the gradient evaluation.

can be performed in parallel easily, which leads to reduced computational cost. In particular, we choose an aggressive agent that continues to place limit orders until the parent order is fulfilled, which results in $T = 5$ in practice. The parametric background agents’ (treated as “reality” in the experiment) configuration is: one Exchange Agent, two Adaptive Market Maker Agents, 100 Value Agents, 25 Momentum Agents, and 5000 Noise Agents; please see Byrd et al. [2020], Amrouni et al. [2021] for additional details on the parametric market simulator ABIDES¹.

Training hyperparameters. As mentioned previously, the number of complete rollout numbers is chosen as $N = 5$ such that the feedback’s empirical distribution under the world agent market is sufficiently different from that of the “real market”. To ensure rollouts under the “real market” will not incur extreme feedback, we conduct $N' = 100$ offline rollouts to construct the feedback collection in reality. As T_0 and b together act like the batch-size, we consider grid search over $T_0 \in \{3, 4, 5\}$ and $b \in \{3, 5\}$. By this grid search, we choose the combination with the smallest (proposed) metric, which is

- $T_0 = 5$ and $b = 3$ for Mkt2NextReturn, which corresponds to the results in Figure 7

¹Available at <https://github.com/jpmorganchase/abides-jpmc-public>

and the **second** column in Figures 8, 18, 9 and 10.

- $T_0 = 5$ and $b = 3$ for `Mkt2NextPriceImpact`, which corresponds to the results in the **forth** column in Figures 8, 18, 9 and 10.

To compare the results of `Mkt2NextReturn` with `EpisodeReward`, we use the same hyperparameter setting for `EpisodeReward`, i.e.,

- $T_0 = 5$ and $b = 3$ for `EpisodeReward`, which corresponds to the results in the **third** column in Figures 8, 18, 9 and 10. The corresponding AT-based metric is optimized from 0.7156 to 0.6176.

Additionally, to further demonstrate of the effectiveness of our AT-based metric and ATMS, we consider

- $T_0 = 2$ and $b = 5$ for `Mkt2NextReturn`, which corresponds to the results in Figure 17.

The initial learning rate r is chosen to be 10^{-9} , which decreases by half every 10 iteration. There are in total 100 iterations and based on the decrease of learning rate they are divided into 10 epochs (each with 10 iterations). We use the cWGAN network parameter trained on AINV market reply data (which is different from the “real” market) as the warm-start/initialization when we train the generator through ATMS.

D.2 Additional results for other feedback candidates

In Figure 14, we present the empirical distribution of other feedback candidates. Interestingly, when utilizing various stylized facts, with the exception of price impact, as the next state, we observe a similar pattern to `EpisodeReward`. This similarity renders these alternatives unfavorable choices in our proposed ATMS and might suggest that those stylized facts are less representative of the market. It is important to mention that we observe a similar pattern of the results for `Mkt2NextPriceImpact` (shown in the last row of Figure 14) to that of our ideal candidate `Mkt2NextReturn` (shown in Figure 4 in the main text of the paper). Therefore, `Mkt2NextPriceImpact` is another candidate that readily be used to train/improve the world agent.

D.3 Additional results for other \hat{d} candidates

In addition to the result for MMD depicted in Figure 6, we present the outcomes for Energy Distance and Earth Mover’s Distance in Figure 15. In the first row where f is chosen as

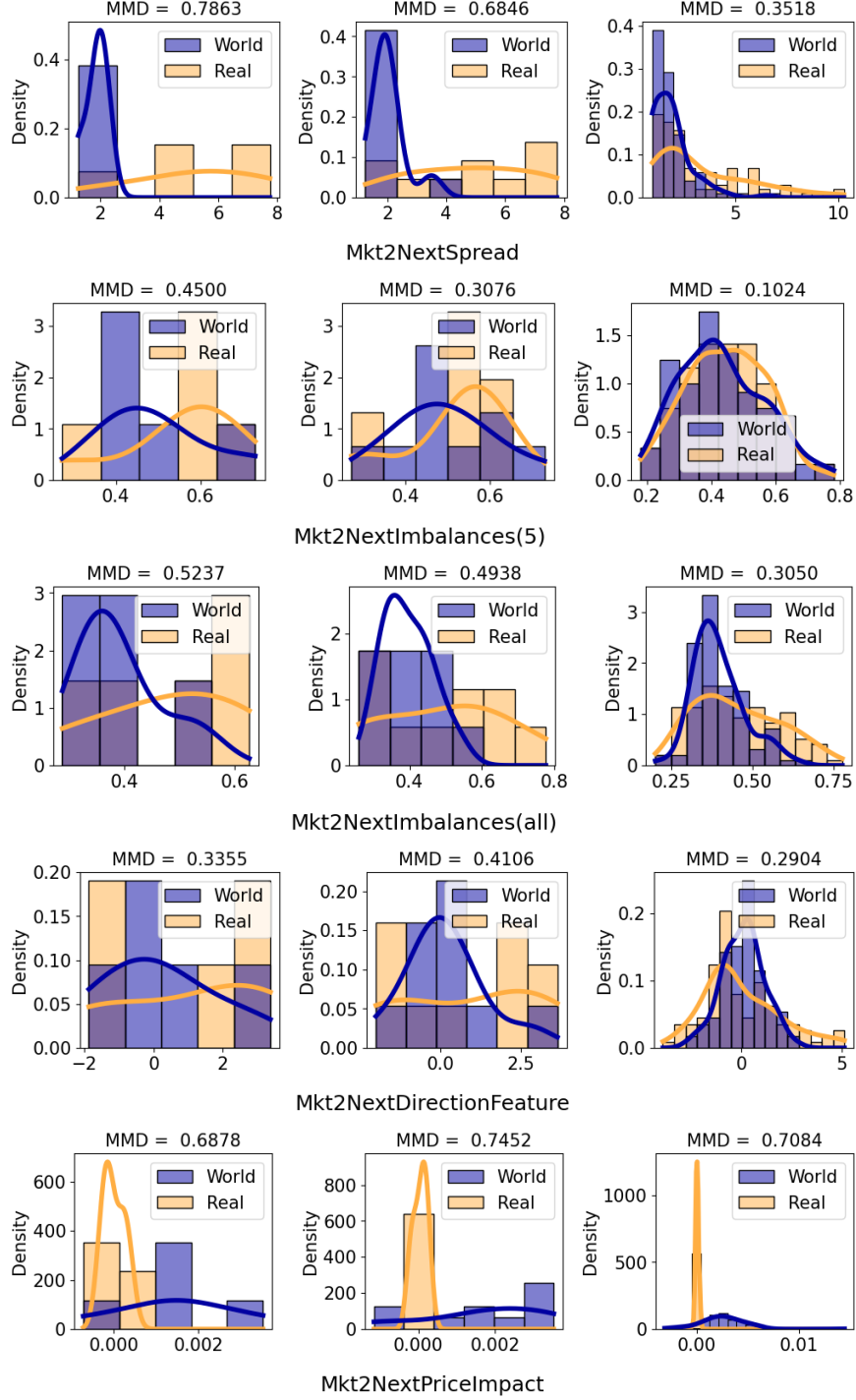


Figure 14: The empirical distribution of additional causal effect feedback candidates (from top to bottom, we report Mkt2NextSpread, Mkt2NextImbalances(5), Mkt2NextImbalances(all), Mkt2NextDirectionFeature, and Mkt2NextPriceImpact) when performing multiple (from left to right: 5, 10, 100) rollouts using AT agent under real (orange) or world agent (blue) markets.

EpisodeReward, we can see the resulting market distance metric’s behavior is reasonable in the sense that the metric is closer to zero when comparing two identical markets (indicated by the orange line, “Real vs Real”). However, the metric performs poorly in differentiating markets as we cannot see the pattern that the blue line is significantly larger than the orange one with a small rollout number (as shown in the right panel in Figure 6).

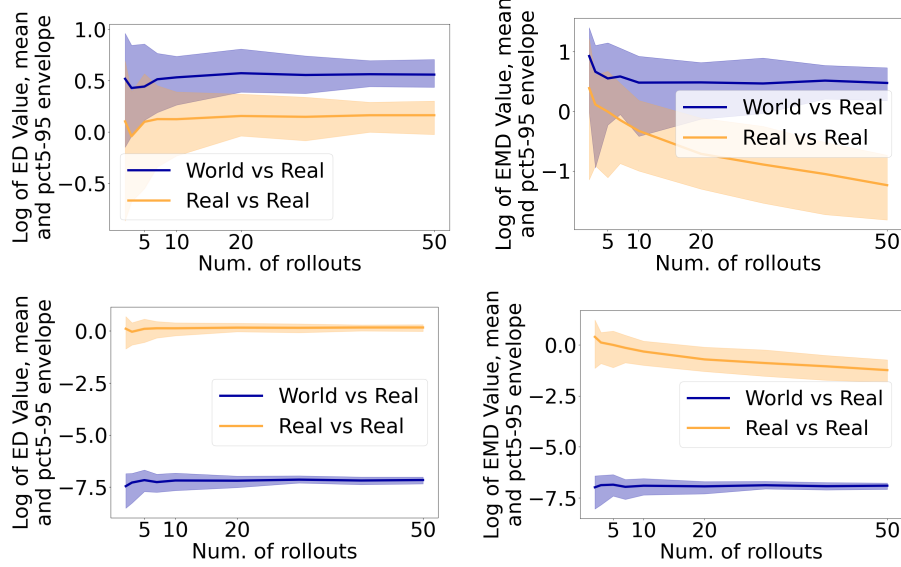


Figure 15: The mean and 5 – 95% envelop trajectory (over 50 bootstrap trials) against increasing number of rollouts of our proposed market distance metric with feedbacks **EpisodeReward** (top) and **Mkt2NextReturn** (bottom), and \hat{d} chosen to be ED (left) and EMD (right).

From the second row in Figure 15, where **Mkt2NextReturn** is chosen as f , it is surprising to find that the metric’s behavior appears unreasonable as the metric between different markets is smaller than that when two markets are identical. The above observations indicate that the corresponding metrics may not be suitable for capturing the dissimilarity (or similarity) between different markets accurately, and therefore ED and EMD are less favorable candidates for the subsequent simulator training.

For completeness and to provide further insights into their unsuitability (for subsequent training of ATMS), we also include the results for MMD, ED, and EMD when choosing **Mkt2Reward** as feedback f in Figure 16. These additional results serve as direct evidence highlighting the undesirable characteristics of these metrics in the context of our ATMS. The findings reinforce the significance of developing and employing a specialized distance metric, as we propose, to effectively evaluate the distance between financial markets, ensuring the reliability of our ATMS.

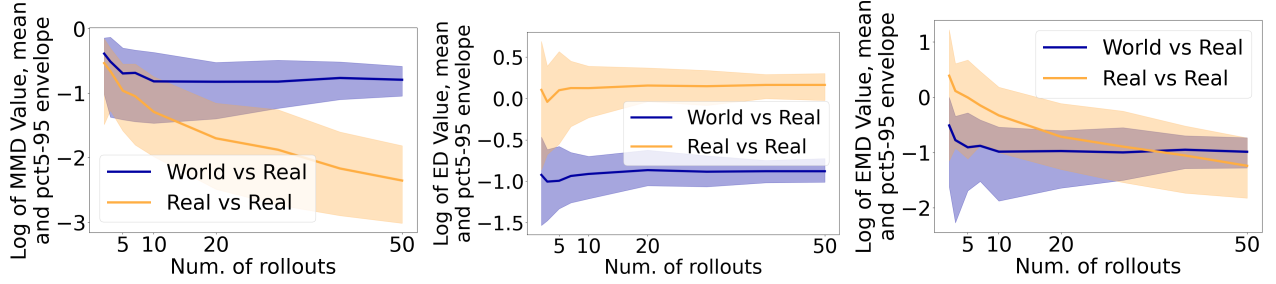


Figure 16: The mean and 5 – 95% envelop trajectory (over 50 bootstrap trials) against increasing number of rollouts of our proposed market distance metric with feedback Mkt2Reward , and \hat{d} chosen to be MMD (left), ED (middle) and EMD (right).

D.4 Additional evidence for the effectiveness of ATMS

To further establish the reliability of our proposed ATMS, we conduct additional experiments to investigate the impact of randomness and training hyperparameters on its effectiveness. In Figure 17, we present the results obtained using a different random seed and distinct training hyperparameters. Remarkably, we observe a similar pattern to the findings depicted in Figure 7. This consistency across different experimental setups strongly suggests that the effectiveness demonstrated in Figure 7 is not solely attributed to randomness but indeed indicative of the superior performance of our proposed ATMS. These findings reinforce the credibility and practical applicability of our ATMS, affirming its capability to consistently generate realistic market data regardless of varying random initialization and training conditions.

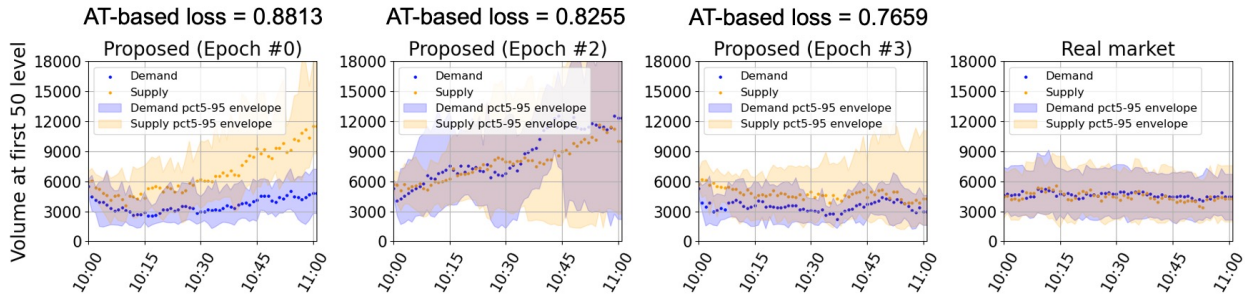


Figure 17: Effectiveness evaluation of our proposed ATMS with different random seeds and training hyperparameters. The consistent pattern across experiments reaffirms the robustness of ATMS in generating realistic market data.

D.5 Additional comparison results of other stylized facts

In the last part, we report results of volume at first n -levels in the LOB for $n \in \{1, 5\}$ in Figure 18, from which we can observe: our proposed approach is behaving similarly to

cWGAN baseline for $n = 1$ case, and they both do not fully capture the real market dynamics; for $n = 5$ case, the patterns are fairly similar to that of $n = 10$ case shown in Figure 8, reaffirming our claims above.

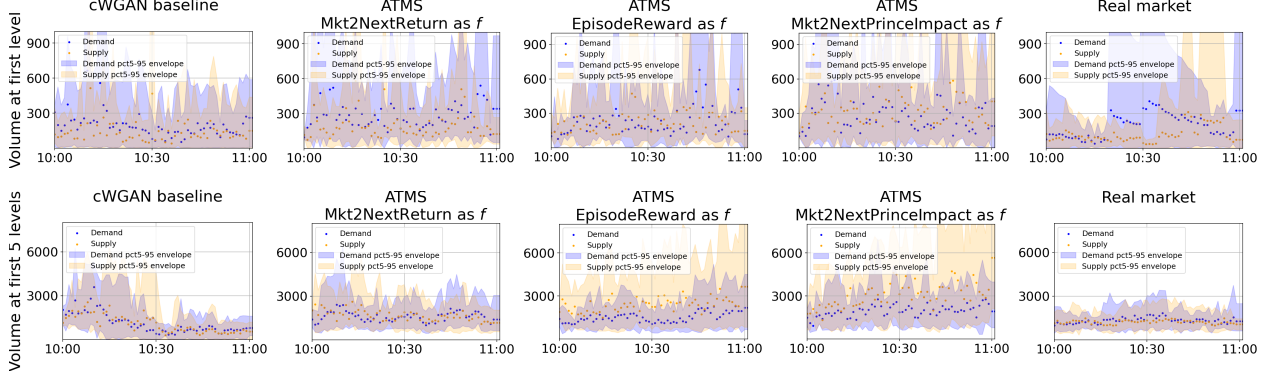


Figure 18: Comparison of volume at first n -levels in the LOB for $n \in \{1, 5\}$ among different simulated markets (specified on top of each panel). We can observe that neither our ATMS nor the cWGAN baseline can correctly capture the volume at the first level whereas our ATMS with Mkt2NextReturn can correctly capture the volume at the first 5-levels (just as shown in Figure 8).